Progress in Fractional Differentiation and Applications
An International Journal

http://dx.doi.org/10.18576/pfda/110409

Numerical Simulations and Analyzing the Dynamics of Hepatitis B Virus With Immune Delay Under Novel Operators

Ali Akgül[1,2,*], *Montasir Qasymeh* [3], *Shabir Ahmad*[4], *Zakaria Che Muda,*[5] *and Nauman Ahmed*[6]

[1] Department of Electronics and Communication Engineering, Saveetha School of Engineering, SIMATS, Chennai, Tamilnadu, India
[2] Department of Mathematics, Art and Science Faculty, Siirt University, TR-56100 Siirt, Turkey
[3] Electrical and Computer Engineering Department, Abu Dhabi University, Abu Dhabi, United Arab Emirates
[4] Department of Mathematics, University of Malakand, Dir(L), Khyber Pakhtunkhwa, Pakistan
[5] Faculty of Engineering and Quantity Surveying, INTI International University, 71800 Nilai, Malaysia
[6] Department of Mathematics and Statistics, The University of Lahore, Lahore, Pakistan

Received: 7 Sept. 2024, Revised: 20 Dec. 2024, Accepted: 21 Feb. 2025
Published online: 1 Oct. 2025

Abstract: Human beings are indeed subject to the hazard of infectious diseases. From the literature, one can see that mathematical modelling is a powerful method for explaining complex biological phenomena accurately. Different operators were used to study the dynamics of infectious diseases. In 2017, more generalized operators are introduced by Atangana through merging fractional and fractal calculus. These newly proposed operators, called fractal-fractional operators, have been commonly utilized to model several physical problems to examine a problem's complex behaviour and complex structure. In this manuscript, the fractal-fractional mathematical model of HBV with an immune delay has investigated qualitatively and quantitatively. The basic reproduction number and equilibria of the proposed model are given. The Routh Hurtwez stability criterion is used to derive the stability of the equilibria points of the model. Fixed point theorems have been used to verify the model's existence and uniqueness when using the Atangana-Baleanu fractal-fractional operator. Non-linear analysis was used to calculate the Ulam-Hyres stability of the model. For the different fractal-fractional operators, numerical results are developed using Lagrangian piecewise interpolation. We visualise the achieved numerical solution for several sets of fractional and fractal orders to examine the dynamic behaviour of the proposed model under novel operators in various ways. This research supports the United Nation SDG 3 (Good Health and Well-Being) by developing a fractal-fractional mathematical model of HBV.

Keywords: Fractal-fractional operators; Ulam-Hyres stability; lagrangian piecewise interpolation, UN SDG 3.

1 Introduction and motivation

Hepatitis B is a life-threatening infection of the liver caused by the hepatitis B virus (HBV). HBV causes mortality and ultimately causes death due to liver diseases. It's among the viruses which severely threaten human health [1,2]. During birth and delivery, the virus is most frequently transmitted from mother to infant, as well as by contact with blood or other body fluids, including contact with an infected partner, injection-drug use involving sharing needles, syringes, or equipment for drug preparation. Statistical regression method [3] and molecular dynamics simulation [4] have been used in predicting the trend and behaviour of the hepatitis virus. In epidemiology, deterministic mathematical models are crucial for evaluating the behaviour of serious diseases. Since then, many articles have been published on modelling of HBV diseases in the last few decades. In related literature, the dynamics and stability of hepatitis B virus from different perspectives and focuses have been studied, but this has been mainly limited to integer-order or delay DEs [5,6,7,8,9]. Recently, the authors in [5] formulated a novel model of HBV infection with immune delay as

* Corresponding author e-mail: aliakgul100727@gmail.com

$$\begin{cases} \frac{d\mathscr{X}}{dt} = \lambda^* - \mu^*\mathscr{X}(t) - \rho\mathscr{X}(t)\mathscr{V}(t) + \sigma^*\mathscr{Y}(t), \\ \frac{d\mathscr{Y}}{dt} = \rho\mathscr{X}(t)\mathscr{V}(t) - (\vartheta + \sigma^*)\mathscr{Y}(t), \\ \frac{d\mathscr{V}}{dt} = c^*\mathscr{Y}(t-\tau)e^{-\kappa\tau} - \gamma^*\mathscr{V}(t). \end{cases} \tag{1}$$

along with initial conditions:

$$\mathscr{X}(0) = \mathscr{X}_0, \mathscr{Y}(0) = \mathscr{Y}_0, \mathscr{V}(0) = \mathscr{V}_0, \tag{2}$$

where $\mathscr{X}(t)$ denotes the concentration of uninfected hepatocytes, $\mathscr{Y}(t)$ represents actively infected hepatocytes and $\mathscr{V}(t)$ represents free virions. Description of the terms of the model are as follows:

–$\lambda^*$is the rate at which uninfected are produced.
–$\mu^*\mathscr{X}(t)$ is the rate at which uninfected hepatocytes are died.
–$\rho\mathscr{X}(t)\mathscr{V}(t)$ is the rate at which uninfected hepatocytes are infected, where ρ is the infection rate constant characteristic of the infection efficiency.
–The rate at which uninfected hepatocytes are produced by cure is denoted by $\vartheta\mathscr{Y}(t)$.
–$\sigma^*\mathscr{Y}(t)$ represents death rate of the infected hepatocytes.
–$c^*\mathscr{Y}(t-\tau)e^{-\kappa\tau}$ represents the production rate of free virions from infected hepatocytes.
–$\gamma^*\mathscr{V}(t)$ denotes the clearance rate of viral particles.
–The time it takes for newly created virions to develop and subsequently become infectious particles is represented by the delay $tau > 0$.
–The probability of immature virions surviving is represented by $e^{-\kappa\tau}$.

Fractional calculus has been used in a variety of applied disciplines, and it has led to a lot of success. In the literature, one can find that three different fractional operators are used for modelling a physical problem. The most basic FO is the Riemann-Liouville and Caputo derivatives (RL) operator which is dependent on the power-law kernel. But some issues were found in this kernel regarding the singularity. This derivative has used for many years and also using nowadays. After a long time, in 2015, another version of the fractional derivative was defined by Caputo and Fabrizio called Caputo-Fabrizio (CF) fractional derivative, which is dependent on the exponential decay kernel. This operator has also some problem regarding the locality of the kernel. To address this issue, in 2016, Atangana and Baleanu defined another type of fractional derivative called the Atangana-Baleanu (AB) fractional derivative, which is dependent on the Mittag-Leffler function. This derivative has extensively used by researchers due to its nonlocal and nonsingular nature. Modelling and simulation utilising these three types of kernels are greatly influenced by the study of fractional-order integrals and differential equations [10,11,12,13,14,15,16,17,18,19]. In comparison to a classical model, a model using FODEs is found to be more accurate. Similarly, there is another concept in differentiation called fractal differentiation, classical differentiation is extended to the concept of fractal differentiation equivalent to the classical derivative if the order of the fractal tends to 1. Many problems in nature are solved by the concept of fractal derivative [20,21]. To generalize the fractional operators, Atangana defined new types of operators with three different kernels which are described above for fractional operators. These operators are called fractal-fractional operators [24]. He merged the fractal derivative and fractional differentiation concepts, accounting for fractal effect, memory, and non-locality. Power-law, forgotten memory, and crossover behaviour problems that are self-similar can all be explained using fractal fractional operators. Classical or FDOs do not capture the complex behaviour of real-world problems, but these operators do. In [22,23,25,26,27], we provide implementations of the novel operators proposed by Atangana. Based on the literature mentioned above, we shall investigate the model (refeq:(1.1)) using several fractal-fractional differential operators.

2 Preliminaries

In over all paper, we will denote the fractional order θ and fractal order by ϖ. For definitions of basic fractal fractional operators, let us assume that $\mathscr{U}(t)$ is fractal differentiable and continuous on (m,n).

Definition 1.*[18] For $0 \leq \theta, \varpi \leq 1$ and power law kernel, the fractal-fractional derivative of $\mathscr{U}(t)$ in Riemann-Liouville sense is defined by:*

$$^{\mathscr{F}\mathscr{F}\mathscr{P}}\mathscr{D}_{0,t}^{\theta,\varpi}(\mathscr{U}(t)) = \frac{1}{\Gamma(w-\theta)}\frac{d}{dt^{\varpi}}\int_0^t (t-\psi)^{w-\theta-1}\mathscr{U}(\psi)d\psi,$$

where $\frac{d}{d\psi^{\varpi}}\mathscr{U}(\psi) = \lim_{t\to\psi}\frac{\mathscr{U}(t)-\mathscr{U}(\psi)}{t^{\varpi}-\psi^{\varpi}}$ *and* $\theta > 0, \varpi \leq w \in \mathbb{N}$.

Definition 2.*[18] For $0 \leq \theta, \varpi \leq 1$ and exponential-decay kernel, the fractal-fractional derivative of $\mathscr{U}(t)$ in Riemann-Liouville sense is defined by:*

$$^{\mathscr{FFE}}\mathscr{D}_{0,t}^{\theta,\varpi}(\mathscr{U}(t)) = \frac{\mathscr{M}(\theta)}{1-\theta}\frac{d}{dt^{\varpi}}\int_0^t \exp\left[-\frac{\theta}{1-\theta}(t-\psi)\right]\mathscr{U}(\psi)d\psi,$$

where $\mathscr{M}(0) = \mathscr{M}(1) = 1$, denotes the normalization function.

Definition 3.*[18] For $0 \leq \theta, \varpi \leq 1$ and Mittag-Leffler kernel, the fractal-fractional derivative of $\mathscr{U}(t)$ in Riemann-Liouville sense is defined by:*

$$^{\mathscr{FFM}}\mathscr{D}_{0,t}^{\theta,\varpi}(\mathscr{U}(t)) = \frac{\mathscr{AB}(\theta)}{1-\theta}\frac{d}{dt^{\varpi}}\int_0^t E_{\theta}\left[-\frac{\theta}{1-\theta}(t-\psi)^{\theta}\right]\mathscr{U}(\psi)d\psi,$$

where $0 < \theta, \varpi \leq 1$ and $\mathscr{AB}(\theta) = 1-\theta+\frac{\theta}{\Gamma(\theta)}$.

Definition 4.*[18] For $0 \leq \theta, \varpi \leq 1$ and power law kernel, the fractal-fractional integral of $\mathscr{U}(t)$ is defined by:*

$$^{\mathscr{FFP}}\mathscr{J}_{0,t}^{\theta,\varpi}\mathscr{U}(t) = \frac{1}{\Gamma\theta}\int_0^t (t-\psi)^{\theta-1}\psi^{1-\varpi}\mathscr{U}(\psi)d\psi.$$

Definition 5.*[18] For $0 \leq \theta, \varpi \leq 1$ and exponential kernel, the fractal-fractional integral of $\mathscr{U}(t)$ is defined by:*

$$^{\mathscr{FFE}}\mathscr{J}_{0,t}^{\theta,\varpi}\mathscr{U}(t) = \frac{\varpi(1-\theta)t^{\varpi-1}\mathscr{U}(t)}{\mathscr{M}(\theta)} + \frac{\theta\varpi}{\mathscr{M}(\theta)}\int_0^t \psi^{\theta-1}\mathscr{U}(\psi)d\psi.$$

Definition 6.*[18] For $0 \leq \theta, \varpi \leq 1$ and Mittag-Leffler kernel, the fractal-fractional integral of $\mathscr{U}(t)$ is defined by:*

$$^{\mathscr{FFM}}\mathscr{J}_{0,t}^{\theta,\varpi}\mathscr{U}(t) = \frac{\varpi(1-\theta)t^{\varpi-1}\mathscr{U}(t)}{\mathscr{AB}(\theta)} + \frac{\theta\varpi}{\mathscr{AB}(\theta)}\int_0^t \psi^{\theta-1}(t-\psi)^{\theta-1}\mathscr{U}(\psi)d\psi.$$

3 Equilibrium points and its stability

Consider the model (1) under fractal-fractional operator as

$$\begin{cases} \mathscr{D}_{0,t}^{\theta,\varpi}\mathscr{X}(t) = \lambda^* - \mu^*\mathscr{X}(t) - \rho\mathscr{X}(t)\mathscr{V}(t) + \sigma^*\mathscr{Y}(t), \\ \mathscr{D}_{0,t}^{\theta,\varpi}\mathscr{Y}(t) = \rho\mathscr{X}(t)\mathscr{V}(t) - (\vartheta+\sigma^*)\mathscr{Y}(t), \\ \mathscr{D}_{0,t}^{\theta,\varpi}\mathscr{V}(t) = c^*\mathscr{Y}(t-\tau)e^{-\kappa\tau} - \gamma^*\mathscr{V}(t), \end{cases} \tag{3}$$

along with the initial conditions (1). The basic reproduction number is given by

$$\mathscr{R}_0 = \frac{\rho\lambda^* c^* e^{-\kappa\tau}}{\gamma^*\mu^*(\vartheta+\sigma^*)}. \tag{4}$$

Now to calculate equilibrium points of the points of the proposed model, put the left hand side ($\mathscr{D}_{0,t}^{\theta,\varpi}(.)$)=0, we obtain the disease free (D_1) and endemic (E_1) eqilibrium points as

$$D_1 = \left(\frac{\lambda^*}{\mu^*}, 0, 0\right), \tag{5}$$

$$E_1 = (\mathscr{X}_1, \mathscr{Y}_1, \mathscr{V}_1), \tag{6}$$

where

$$\begin{cases} \mathscr{X}_1 = \frac{\lambda^*}{\mu^*\mathscr{R}_0}, \\ \mathscr{Y}_1 = \frac{\lambda^*}{\vartheta\mathscr{R}_0}(\mathscr{R}_0 - 1), \\ \mathscr{V}_1 = \frac{\lambda^* c^* e^{-\kappa\tau}}{\vartheta\gamma^*}(\mathscr{R}_0 - 1). \end{cases} \tag{7}$$

Theorem 1.*The suggested model (3) is locally asymptotically stable (LAS) at D_1, if $\mathscr{R}_0 < 1$, otherwise unstable*

*Proof.*We write the Jacobian matrix at D_1 is as:

$$J(D_1)=\begin{bmatrix}-\mu^* & \sigma^* & 0\\ 0 & -(\vartheta+\sigma^*) & 0\\ 0 & c^*e^{-\kappa\tau} & -\gamma^*\end{bmatrix},$$

after doing some calculation, we find the eigenvalues of the above matrix as $\lambda_1=-\gamma^*,\lambda_2=-\mu^*,\lambda_3=-(\vartheta+\sigma^*)$. We see that all eigen values are negative. Hence the disease free equilibrium point D_1 is LAS.

Theorem 2.*The proposed model (3) is locally asymptotically stable (LAS) at E_1, if $\mathscr{R}_0>1$, otherwise unstable*

*Proof.*The Jacobian matrix at E_1 is

$$J(E_1)=\begin{bmatrix}-\mu^*-\rho\mathscr{V}_1 & \sigma^* & -\rho\mathscr{X}_1\\ \rho\mathscr{V}_1 & -(\vartheta+\sigma^*) & \rho\mathscr{X}_1\\ 0 & c^*e^{-\kappa\tau} & -\gamma^*\end{bmatrix},$$

now to find eigen values put $|J(E_1)-\lambda|=0$. After some manipulation, we get

$$\lambda^3+a_2\lambda^2+a_1\lambda+a_0=0,$$

where

$$\begin{cases}a_2 &= (\vartheta+\sigma^*+\gamma^*)+\rho\mathscr{X}_1c^*e^{-\kappa\tau},\\ a_1 &= (\vartheta+\sigma^*)\gamma^*+(\mu^*+\rho\mathscr{V}_1)(\vartheta+\sigma^*+\gamma^*)-\rho\mathscr{X}_1c^*e^{-\kappa\tau}-\rho\mathscr{V}_1\sigma^*,\\ a_0 &= \rho^2\mathscr{V}_1\mathscr{X}_1c^*e^{-\kappa\tau}+\gamma^*(\mu^*+\rho\mathscr{V}_1)(\vartheta+\sigma^*)\\ &\quad -\rho\mathscr{X}_1c^*e^{-\kappa\tau}(\mu^*+\rho\mathscr{V}_1)-\rho\mathscr{V}_1\sigma^*\gamma^*.\end{cases}$$

Since $\mathscr{R}_0>1$,then using the Routh–Hurwitz stability criterion of 3^{rd} order, the constraint hold $a_0>0,a_2>0$,and $a_2a_1>a_0$. Thus, the endemic equilibrium point $E_1$is LAS.

4 Theoretical analysis

We will study the model's under the consideration qualitatively in this section. We will present the existence and uniquness results and Ulam-Hyres type stability of the model under consideration under novel operators in AB sense. One can derive the same results for the Caputo and CF fractal -fractional model of (1). Consider

$$\begin{cases}{}^{\mathscr{FFM}}\mathscr{D}_{0,t}^{\theta,\varpi}\mathscr{X}(t)=\lambda^*-\mu^*\mathscr{X}(t)-\rho\mathscr{X}(t)\mathscr{V}(t)+\sigma^*\mathscr{Y}(t),\\ {}^{\mathscr{FFM}}\mathscr{D}_{0,t}^{\theta,\varpi}\mathscr{Y}(t)=\rho\mathscr{X}(t)\mathscr{V}(t)-(\vartheta+\sigma^*)\mathscr{Y}(t),\\ {}^{\mathscr{FFM}}\mathscr{D}_{0,t}^{\theta,\varpi}\mathscr{V}(t)=c^*\mathscr{Y}(t-\tau)e^{-\kappa\tau}-\gamma^*\mathscr{V}(t).\end{cases}$$

4.1 Existence and uniqueness results

Using fixed point results, we show that the model under study has at least one and only one solution. We may formulate the proposed model as follows because the integral is differentiable.

$$\begin{cases}{}^{ABR}_{0}D_t^{\theta}\mathscr{X}(t)=\varpi t^{\varpi-1}\mathscr{Q}(t,\mathscr{X},\mathscr{Y},\mathscr{V}),\\ {}^{ABR}_{0}D_t^{\theta}\mathscr{Y}(t)=\varpi t^{\varpi-1}\mathscr{W}(t,\mathscr{X},\mathscr{Y},\mathscr{V}),\\ {}^{ABR}_{0}D_t^{\theta}\mathscr{V}(t)=\varpi t^{\varpi-1}\mathscr{E}(t,\mathscr{X},\mathscr{Y},\mathscr{V}),\end{cases}\tag{8}$$

where

$$\begin{cases}\mathscr{Q}(t,\mathscr{X},\mathscr{Y},\mathscr{V})=\lambda^*-\mu^*\mathscr{X}(t)-\rho\mathscr{X}(t)\mathscr{V}(t)+\sigma^*\mathscr{Y}(t),\\ \mathscr{W}(t,\mathscr{X},\mathscr{Y},\mathscr{V})=\rho\mathscr{X}(t)\mathscr{V}(t)-(\vartheta+\sigma^*)\mathscr{Y}(t),\\ \mathscr{E}(t,\mathscr{X},\mathscr{Y},\mathscr{V})=c^*\mathscr{Y}(t-\tau)e^{-\kappa\tau}-\gamma^*\mathscr{V}(t).\end{cases}$$

We can write system (8) as:

$$\begin{cases} {}_0^{ABR}D_t^{\theta}\Upsilon(t) = \varpi t^{\varpi-1}\Lambda\left(t,\Upsilon(t)\right), \\ \Upsilon(0) = \Upsilon_0. \end{cases} \tag{9}$$

By replacing ${}_0^{ABR}D_t^{\theta,\varpi}$ by ${}_0^{ABC}D_t^{\theta,\varpi}$ and using corresponding integral, we get

$$\Upsilon(t) = \Upsilon(0) + \frac{\varpi t^{\varpi-1}(1-\theta)}{AB(\theta)}\Lambda\left(t,\Pi(t)\right) + \frac{\theta\varpi}{AB(\theta)\Gamma(\theta)}\int_0^t \lambda^{\varpi-1}(t-\lambda)^{\varpi-1}\Lambda\left(\lambda,\Upsilon(\lambda)\right)d\lambda,$$

where $\Upsilon(t) = \begin{cases} \mathscr{X}(t) \\ \mathscr{Y}(t) \\ \mathscr{V}(t) \end{cases}, \Upsilon(0) = \begin{cases} \mathscr{X}(0) \\ \mathscr{Y}(0) \\ \mathscr{V}(0) \end{cases}, \Lambda\left(t,\Upsilon(t)\right) = \begin{cases} \mathscr{Q}(t,\mathscr{X},\mathscr{Y},\mathscr{V}) \\ \mathscr{W}(t,\mathscr{X},\mathscr{Y},\mathscr{V}) \\ \mathscr{E}(t,\mathscr{X},\mathscr{Y},\mathscr{V}) \end{cases}$ For the our analysis, let us take a Banach space $\mathfrak{B} = \mathscr{C}\times\mathscr{C}\times\mathscr{C}$, where $\mathscr{C} = \mathbb{C}[0,\mathbb{T}]$ under the norm

$$\|\Upsilon\| = \max_{t\in[0,\mathbb{T}]}\left|\mathscr{X}(t)+\mathscr{Y}(t)+\mathscr{V}(t)\right|.$$

We define an operator $\Omega : \mathfrak{B}\to\mathfrak{B}$as:

$$\Omega(\Upsilon)(t) = \Upsilon(0) + \frac{\varpi t^{\varpi-1}(1-\theta)}{AB(\theta)}\Lambda\left(t,\Upsilon(t)\right) + \frac{\theta\varpi}{AB(\theta)\Gamma(\theta)}\int_0^t \lambda^{\varpi-1}(t-\lambda)^{\varpi-1}\Lambda\left(\lambda,\Upsilon(\lambda)\right)d\lambda. \tag{10}$$

We take some conditions for nonlinear function $\Lambda\left(t,\Upsilon(t)\right)$ which are given below:

–For every $\Upsilon\in\mathfrak{B}$,$\exists$ positive constants $\mathscr{C}_\Lambda$ and M_Λ which holds:

$$\left|\Lambda\left(t,\Upsilon(t)\right)\right| \le \mathscr{C}_\Lambda\left|\Upsilon(t)\right| + M_\Lambda, \tag{11}$$

–For every $\Upsilon,\overline{\Upsilon}\in\mathfrak{B}$,$\exists\ \mathscr{L}_\Lambda > 0$ such that

$$\left|\Lambda\left(t,\Upsilon(t)\right) - \Lambda\left(t,\overline{\Upsilon}(t)\right)\right| \le \mathscr{L}_\Lambda\left|\Upsilon(t)-\overline{\Upsilon}(t)\right|. \tag{12}$$

Theorem 3.*Presume that (11) holds and $\Lambda : [0,\mathbb{T}]\times\mathfrak{B}\to\mathbb{R}$ be a continuous mapping. Then at least one solution exists for the suggested model.*

*Proof.*To begin, we must demonstrate that the operator Ω defined by (10) is completely continuous. Because Λ is continuous, so Ω is as well. Let $\mathbb{H} = \{\Upsilon\in\mathfrak{B} : \|\Upsilon\|\le\mathscr{R},\mathscr{R}>0\}$. Now for any $\Upsilon\in\mathfrak{B}$, we have

$$\begin{aligned}
\|\Omega(\Upsilon)\| = \max_{t\in[0,\mathbb{T}]}\Bigg|&\Upsilon(0) + \frac{\varpi t^{\varpi-1}(1-\theta)}{AB(\theta)}\Lambda\left(t,\Upsilon(t)\right) \\
&+ \frac{\theta\varpi}{AB(\theta)\Gamma(\theta)}\int_0^t \lambda^{\varpi-1}(t-\lambda)^{\varpi-1}\Lambda\left(\lambda,\Upsilon(\lambda)\right)d\lambda\Bigg| \\
\le&\Upsilon(0) + \frac{\varpi\mathbb{T}^{\varpi-1}(1-\theta)}{AB(\theta)}\left(\mathscr{C}_\Lambda\|\Upsilon\| + M_\Lambda\right) \\
&+ \max_{t\in[0,\mathbb{T}]}\frac{\theta\varpi}{AB(\theta)\Gamma(\theta)}\int_0^t \lambda^{\varpi-1}(t-\lambda)^{\varpi-1}\left|\Lambda\left(\lambda,\Upsilon(\lambda)\right)\right|d\lambda \\
\le&\Upsilon(0) + \frac{\varpi\mathbb{T}^{\varpi-1}(1-\theta)}{AB(\theta)}\left(\mathscr{C}_\Lambda\|\Upsilon\| + M_\Lambda\right) \\
&+ \frac{\theta\varpi}{AB(\theta)\Gamma(\theta)}\left(\mathscr{C}_\Lambda\|\Upsilon\| + M_\Lambda\right)\mathbb{T}^{\theta+\varpi-1}\mathscr{H}(\theta,\varpi) \\
\le&\mathscr{R},
\end{aligned}$$

where $\mathscr{H}(\theta,\varpi)$ represents the beta function. Thus, from the last inequality, Ω is uniformly bounded. Next for $t_1 < t_2 \leq \mathbb{T}$, consider

$$\begin{aligned}|\Omega(\Upsilon)(t_2)-\Omega(\Upsilon)(t_1)| = &\left| \frac{\varpi t_2^{\varpi-1}(1-\theta)}{AB(\theta)}\Lambda\left(t_2,\Upsilon(t_2)\right)+\frac{\theta\varpi}{AB(\theta)\Gamma(\theta)}\int_0^{t_2}\lambda^{\varpi-1}(t_2-\lambda)^{\varpi-1}\Lambda\left(\lambda,\Upsilon(\lambda)\right)d\lambda\right.\\ &\left.-\frac{\varpi t_1^{\varpi-1}(1-\theta)}{AB(\theta)}\Lambda\left(t_1,\Upsilon(t_1)\right)+\frac{\theta\varpi}{AB(\theta)\Gamma(\theta)}\int_0^{t_1}\lambda^{\varpi-1}(t_1-\lambda)^{\varpi-1}\Lambda\left(\lambda,\Upsilon(\lambda)\right)d\lambda\right|\\ \leq &\frac{\varpi t_2^{\varpi-1}(1-\theta)}{AB(\theta)}\left(\mathscr{C}_\Lambda|\Upsilon(t)|+M_\Lambda\right)+\frac{\theta\varpi}{AB(\theta)\Gamma(\theta)}\left(\mathscr{C}_\Lambda|\Upsilon(t)|+M_\Lambda\right)t_2^{\theta+\varpi-1}\mathscr{H}(\theta,\varpi)\\ &-\frac{\varpi t_1^{\varpi-1}(1-\theta)}{AB(\theta)}\left(\mathscr{C}_\Lambda|\Upsilon(t)|+M_\Lambda\right)-\frac{\theta\varpi}{AB(\theta)\Gamma(\theta)}\left(\mathscr{C}_\Lambda|\Upsilon(t)|+M_\Lambda\right)t_1^{\theta+\varpi-1}\mathscr{H}(\theta,\varpi),\end{aligned}$$

if $t_1 \to t_2$,then $|\Omega(\Upsilon)(t_2)-\Omega(\Upsilon)(t_1)| \to 0$. It follows that

$$\|\Omega(\Upsilon)(t_2)-\Omega(\Upsilon)(t_1)\| \to 0, \quad \text{as } t_1 \to t_2.$$

It follows that Ω is equicontinuous. As a result, the Arzela-Ascoli theorem states that it is absolutely continuous. Therefore, the proposed model has at least one solution, according to Schauder's fixed point result.

Theorem 4.*Presume that (12) satisfies and*

$$\rho = \left(\frac{\varpi\mathbb{T}^{\varpi-1}(1-\theta)}{AB(\theta)}+\frac{\theta\varpi}{AB(\theta)\Gamma(\theta)}\mathbb{T}^{\theta+\varpi-1}\mathscr{H}(\theta,\varpi)\right)\mathscr{L}_\Lambda < 1,$$

then unique solution the considered model will be exist.

*Proof.*For $\Upsilon,\overline{\Upsilon} \in \mathfrak{B}$,we have

$$\begin{aligned}\left\|\Omega(\Upsilon)-\Omega(\overline{\Upsilon})\right\| = &\max_{t\in[0,\mathbb{T}]}\left|\frac{\varpi t^{\varpi-1}(1-\theta)}{AB(\theta)}\left(\Lambda\left(t,\Upsilon(t)\right)-\Lambda\left(t,\overline{\Upsilon}(t)\right)\right)\right.\\ &\left.+\frac{\theta\varpi}{AB(\theta)\Gamma(\theta)}\int_0^t\lambda^{\varpi-1}(t-\lambda)^{\varpi-1}d\lambda\left[\Lambda\left(\lambda,\Upsilon(\lambda)\right)-\Lambda\left(\lambda,\overline{\Upsilon}(\lambda)\right)\right]\right|\\ \leq &\left[\frac{\varpi\mathbb{T}^{\varpi-1}(1-\theta)}{AB(\theta)}+\frac{\theta\varpi}{AB(\theta)\Gamma(\theta)}\mathbb{T}^{\theta+\varpi-1}\mathscr{H}(\theta,\varpi)\right]\left\|\Upsilon-\overline{\Upsilon}\right\|\\ \leq &\rho\left\|\Upsilon-\overline{\Upsilon}\right\|\end{aligned}$$

Thus Ω satisfies the contraction condition. The model's under consideration possesses a unique solution as a result of the Banach contraction theorem.

4.2 Ulam-Hyres type stability

The suggested model's Ulam-Hyres stability will be demonstrated in this section.

Definition 7.*The model under consideration is Ulam-Hyres stable if* $\exists\ \Omega_{\theta,\varpi} \geq 0$, *for any* $\varepsilon > 0$ *and for every* $\Upsilon \in \mathbb{C}([0,\mathbb{T}],\mathbb{R})$ *holds inequality as follows:*

$$\left|{}_0^{FFM}D_t^{\theta,\varpi}\Upsilon(t)-\Lambda\left(t,\Upsilon(t)\right)\right| \leq \varepsilon,\ t\in[0,\mathbb{T}],$$

and $\exists$ *a unique solution* $\Omega \in \mathbb{C}([0,\mathbb{T}],\mathbb{R})$ *such that*

$$|\Upsilon(t)-\Omega(t)| \leq \Omega_{\theta,\varpi}\varepsilon, \quad t\in[0,\mathbb{T}].$$

Let $\Phi \in \mathbb{C}[0,\mathbb{T}]$ be a small perturbation such that $\Phi(0)=0$. Let

– $|\Phi(t)| \leq \varepsilon$,for $\varepsilon > 0$.

– ${}_0^{FFM}D_t^{\theta,\varpi}\Upsilon(t) = \Lambda(t,\Upsilon(t)) + \Phi(t)$.

Lemma 1.*The solution to the following model*

$$\begin{aligned} {}_0^{FFM}D_t^{\theta,\varpi}\Upsilon(t) &= \Lambda(t,\Upsilon(t)) + \Phi(t) \\ \Upsilon(0) &= \Upsilon_0 \end{aligned}$$

satisfies the following inequality

$$\left|\Upsilon(t) - \left(\Upsilon(0) + \frac{\varpi t^{\varpi-1}(1-\theta)}{AB(\theta)}\Lambda(t,\Upsilon(t)) + \frac{\theta\varpi}{AB(\theta)\Gamma(\theta)}\int_0^t \lambda^{\varpi-1}(t-\lambda)^{\varpi-1}\Lambda(\lambda,\Upsilon(\lambda))d\lambda\right)\right| \leq \Theta_{\theta,\varpi}\varepsilon$$

where $\Theta_{\theta,\varpi} = \frac{\varpi\mathbb{T}^{\varpi-1}(1-\theta)}{AB(\theta)} + \frac{\theta\varpi}{AB(\theta)\Gamma(\theta)}\mathbb{T}^{\theta+\varpi-1}\mathscr{H}(\theta,\varpi)$

*Proof.*The proof is straightforward.

Lemma 2.*Assume that (12) holds and considering the Lemma (1), the solution of the considered model is Ulam-Hyres stable if* $\rho < 1$.

*Proof.*Let a unique solution of the model is $\Omega \in \mathfrak{B}$ and and any other solution is $\Upsilon \in \mathfrak{B}$, then

$$\begin{aligned} &|\Upsilon(t)-\Omega(t)| \\ &= \left|\Upsilon(t) - \left[\Omega(0) + \frac{\varpi t^{\varpi-1}(1-\theta)}{AB(\theta)}\Lambda(t,\Omega(t)) \right.\right. \\ &\quad \left.\left. + \frac{\theta\varpi}{AB(\theta)\Gamma(\theta)}\int_0^t \lambda^{\varpi-1}(t-\lambda)^{\varpi-1}\Lambda(\lambda,\Omega(\lambda))d\lambda\right]\right| \\ &\leq \left|\Upsilon(t) - \left(\Upsilon(0) + \frac{\varpi t^{\varpi-1}(1-\theta)}{AB(\theta)}\Lambda(t,\Upsilon(t)) + \frac{\theta\varpi}{AB(\theta)\Gamma(\theta)}\int_0^t \lambda^{\varpi-1}(t-\lambda)^{\varpi-1}\Lambda(\lambda,\Upsilon(\lambda))d\lambda\right)\right| \\ &\quad + \left|\Upsilon(0) + \frac{\varpi t^{\varpi-1}(1-\theta)}{AB(\theta)}\Lambda(t,\Upsilon(t)) + \frac{\theta\varpi}{AB(\theta)\Gamma(\theta)}\int_0^t \lambda^{\varpi-1}(t-\lambda)^{\varpi-1}\Lambda(\lambda,\Upsilon(\lambda))d\lambda\right| \\ &\quad - \left|\Omega(0) + \frac{\varpi t^{\varpi-1}(1-\theta)}{AB(\theta)}\Lambda(t,\Omega(t)) + \frac{\theta\varpi}{AB(\theta)\Gamma(\theta)}\int_0^t \lambda^{\varpi-1}(t-\lambda)^{\varpi-1}\Lambda(\lambda,\Omega(\lambda))d\lambda\right| \\ &\leq \Theta_{\theta,\varpi}\varepsilon + \left(\frac{\varpi\mathbb{T}^{\varpi-1}(1-\theta)}{AB(\theta)} + \frac{\theta\varpi}{AB(\theta)\Gamma(\theta)}\mathbb{T}^{\theta+\varpi-1}\mathscr{H}(\theta,\varpi)\right)\mathscr{L}_\Lambda|\Upsilon(t)-\Omega(t)| \\ &\leq \Theta_{\theta,\varpi}\varepsilon + \rho|\Upsilon(t)-\Omega(t)|. \end{aligned}$$

It follows that

$$\|\Upsilon-\Omega\| \leq \Theta_{\theta,\varpi}\varepsilon + \rho\|\Upsilon-\Omega\|$$

This implies that

$$\|\Upsilon-\Omega\| \leq \Omega_{\theta,\varpi}\varepsilon$$

where $\Omega_{\theta,\varpi} = \frac{\Theta_{\theta,\varpi}}{1-\rho}$. As a result, the suggested problem's solution is Ulam-Hyres stable.

5 Numerical Schemes

We will use Lagrangian piece wise interpolation to build numerical schemes for the proposed model under the Caputo, CF, and AB fractal-fractional operators in this section.

5.1 Numerical scheme for Caputo operator

In this part, we derive a numerical scheme of the model (1) under the novel operator in Caputo sense. Consider (1) as

$$\begin{cases} {}^{\mathscr{FFP}}\mathscr{D}_{0,t}^{\theta,\varpi}\mathscr{X}(t) = \lambda^* - \mu^*\mathscr{X}(t) - \rho\mathscr{X}(t)\mathscr{V}(t) + \sigma^*\mathscr{Y}(t), \\ {}^{\mathscr{FFP}}\mathscr{D}_{0,t}^{\theta,\varpi}\mathscr{Y}(t) = \rho\mathscr{X}(t)\mathscr{V}(t) - (\vartheta+\sigma^*)\mathscr{Y}(t), \\ {}^{\mathscr{FFP}}\mathscr{D}_{0,t}^{\theta,\varpi}\mathscr{V}(t) = c^*\mathscr{Y}(t-\tau)e^{-\kappa\tau} - \gamma^*\mathscr{V}(t). \end{cases} \tag{13}$$

The above equation (13) can be converted to Volterra case by applying ${}^{\mathscr{FFP}}\mathscr{J}_{0,t}^{\theta,\varpi}$ on both sides of equation 13. Since the fractional integral is differentiable then the proposed model can be written as

$$\begin{cases} {}^{\mathscr{RL}}\mathscr{D}_{0,t}^{\theta}\mathscr{X}(t) = \varpi t^{\varpi-1}\left[\lambda^* - \mu^*\mathscr{X}(t) - \rho\mathscr{X}(t)\mathscr{V}(t) + \sigma^*\mathscr{Y}(t)\right], \\ {}^{\mathscr{RL}}\mathscr{D}_{0,t}^{\theta}\mathscr{Y}(t) = \varpi t^{\varpi-1}\left[\rho\mathscr{X}(t)\mathscr{V}(t) - (\vartheta+\sigma^*)\mathscr{Y}(t)\right], \\ {}^{\mathscr{RL}}\mathscr{D}_{0,t}^{\theta}\mathscr{V}(t) = \varpi t^{\varpi-1}\left[c^*\mathscr{Y}(t-\tau)e^{-\kappa\tau} - \gamma^*\mathscr{V}(t)\right]. \end{cases} \tag{14}$$

Now, we replace the $\mathscr{RL}$ derivative by Caputo derivative in order to make the use of the integer-order initial conditions. Then, applying the fractional integral on both sides we have

$$\begin{cases} \mathscr{X}(t) &= \mathscr{X}(0) + \frac{\varpi}{\Gamma(\theta)}\int_0^t \psi^{\varpi-1}(t-\psi)^{\theta-1}\mathscr{H}_1(\psi,\mathscr{X},\mathscr{Y},\mathscr{V})d\psi, \\ \mathscr{Y}(t) &= \mathscr{Y}(0) + \frac{\varpi}{\Gamma(\theta)}\int_0^t \psi^{\varpi-1}(t-\psi)^{\theta-1}\mathscr{H}_2(\psi,\mathscr{X},\mathscr{Y},\mathscr{V})d\psi, \\ \mathscr{V}(t) &= \mathscr{V}(0) + + \frac{\varpi}{\Gamma(\theta)}\int_0^t \psi^{\varpi-1}(t-\psi)^{\theta-1}\mathscr{H}_3(\psi,\mathscr{X},\mathscr{Y},\mathscr{V})d\psi. \end{cases} \tag{15}$$

where

$$\begin{cases} \mathscr{H}_1(\psi,\mathscr{X},\mathscr{Y},\mathscr{V}) = \lambda^* - \mu^*\mathscr{X}(\psi) - \rho\mathscr{X}(\psi)\mathscr{V}(\psi) + \sigma^*\mathscr{Y}(\psi), \\ \mathscr{H}_2(\psi,\mathscr{X},\mathscr{Y},\mathscr{V}) = \rho\mathscr{X}(\psi)\mathscr{V}(\psi) - (\vartheta+\sigma^*)\mathscr{Y}(\psi), \\ \mathscr{H}_3(\psi,\mathscr{X},\mathscr{Y},\mathscr{V}) = c^*\mathscr{Y}(\psi-\tau)e^{-\kappa\tau} - \gamma^*\mathscr{V}(\psi), \end{cases} \tag{16}$$

we now derive the numerical scheme of the above system at the point $t = t_{b+1}$. The system (15) takes the form:

$$\begin{cases} \mathscr{X}^{b+1} &= \mathscr{X}^0 + \frac{\varpi}{\Gamma(\theta)}\int_0^{t_{b+1}} \psi^{\varpi-1}(t_{b+1}-\psi)^{\theta-1}\mathscr{H}_1(\psi,\mathscr{X},\mathscr{Y},\mathscr{V})d\psi, \\ \mathscr{Y}^{b+1} &= \mathscr{Y}^0 + \frac{\varpi}{\Gamma(\theta)}\int_0^{t_{b+1}} \psi^{\varpi-1}(t_{b+1}-\psi)^{\theta-1}\mathscr{H}_2(\psi,\mathscr{X},\mathscr{Y},\mathscr{V})d\psi, \\ \mathscr{V}^{b+1} &= \mathscr{V}^0 + + \frac{\varpi}{\Gamma(\theta)}\int_0^{t_{b+1}} \psi^{\varpi-1}(t_{b+1}-\psi)^{\theta-1}\mathscr{H}_3(\psi,\mathscr{X},\mathscr{Y},\mathscr{V})d\psi. \end{cases} \tag{17}$$

Then the approximation of the above system is given below:

$$\begin{cases} \mathscr{X}^{b+1} &= \mathscr{X}^0 + \frac{\varpi}{\Gamma(\theta)}\sum_{s=0}^{b}\int_{t_s}^{t_{s+1}} \psi^{\varpi-1}(t_{b+1}-\psi)^{\theta-1}\mathscr{H}_1(\psi,\mathscr{X},\mathscr{Y},\mathscr{V})d\psi, \\ \mathscr{Y}^{b+1} &= \mathscr{Y}^0 + \frac{\varpi}{\Gamma(\theta)}\sum_{s=0}^{b}\int_{t_s}^{t_{s+1}} \psi^{\varpi-1}(t_{b+1}-\psi)^{\theta-1}\mathscr{H}_2(\psi,\mathscr{X},\mathscr{Y},\mathscr{V})d\psi, \\ \mathscr{V}^{b+1} &= \mathscr{V}^0 + + \frac{\varpi}{\Gamma(\theta)}\sum_{s=0}^{b}\int_{t_s}^{t_{s+1}} \psi^{\varpi-1}(t_{b+1}-\psi)^{\theta-1}\mathscr{H}_3(\psi,\mathscr{X},\mathscr{Y},\mathscr{V})d\psi. \end{cases} \tag{18}$$

We approximate the function $\psi^{\varpi-1}\mathscr{H}_1(\psi,\mathscr{X},\mathscr{Y},\mathscr{V})$ with aid of Lagrangian piece-wise interpolation in $[t_s, t_{s+1}]$ as follows:

$$\begin{cases} \mathscr{P}_s(\psi) &= \frac{\psi-t_{s-1}}{t_s-t_{s-1}}t_s^{\varpi-1}\mathscr{H}_1(t^s,\mathscr{X}^s,\mathscr{Y}^s,\mathscr{V}^s) \\ &\quad -\frac{\psi-t_s}{t_s-t_{s-1}}t_{s-1}^{\varpi-1}\mathscr{H}_1(t^{s-1},\mathscr{X}^{s-1},\mathscr{Y}^{s-1},\mathscr{V}^{s-1}), \\ \mathscr{Q}_s(\psi) &= \frac{\psi-t_{s-1}}{t_s-t_{s-1}}t_s^{\varpi-1}\mathscr{H}_2(t^s,\mathscr{X}^s,\mathscr{Y}^s,\mathscr{V}^s) \\ &\quad -\frac{\psi-t_s}{t_s-t_{s-1}}t_{j-1}^{\varpi-1}\mathscr{H}_2(t^{s-1},\mathscr{X}^{s-1},\mathscr{Y}^{s-1},\mathscr{V}^{s-1}), \\ \mathscr{R}_s(\psi) &= \frac{\psi-t_{s-1}}{t_s-t_{s-1}}t_j^{\varpi-1}\mathscr{H}_3(t^s,\mathscr{X}^s,\mathscr{Y}^s,\mathscr{V}^s) \\ &\quad -\frac{\psi-t_s}{t_s-t_{s-1}}t_{j-1}^{\varpi-1}\mathscr{H}_3(t^{s-1},\mathscr{X}^{s-1},\mathscr{Y}^{s-1},\mathscr{V}^{s-1}). \end{cases} \tag{19}$$

Thus, the system (18) becomes

$$\begin{cases} \mathscr{X}^{b+1} &= \mathscr{X}^0 + \frac{\varpi}{\Gamma(\theta)} \sum_{s=0}^{b} \int_{t_s}^{t_{s+1}} \psi^{\varpi-1}(t_{b+1}-\psi)^{\theta-1} \mathscr{P}_s(\psi) d\psi, \\ \mathscr{Y}^{b+1} &= \mathscr{Y}^0 + \frac{\varpi}{\Gamma(\theta)} \sum_{s=0}^{b} \int_{t_s}^{t_{s+1}} \psi^{\varpi-1}(t_{b+1}-\psi)^{\theta-1} \mathscr{Q}_s(\psi) d\psi, \\ \mathscr{V}^{b+1} &= \mathscr{V}^0 + + \frac{\varpi}{\Gamma(\theta)} \sum_{s=0}^{b} \int_{t_s}^{t_{s+1}} \psi^{\varpi-1}(t_{b+1}-\psi)^{\theta-1} \mathscr{R}_s(\psi) d\psi. \end{cases} \tag{20}$$

Solving the integrals of the right hand sides, we obtain the following numerical scheme

$$\begin{cases} \mathscr{X}^{b+1} &= \mathscr{X}^0 + \frac{\varpi(\Delta t)^\theta}{\Gamma(\theta+2)} \sum_{s=0}^{b} \left[t_{s-1}^{\varpi} \mathscr{H}_1(t_s, \mathscr{X}^s, \mathscr{Y}^s, \mathscr{V}^s) \right. \\ & \times \left((-s+b+1)^\theta (-s+\theta+b+2) - (b-s)^\theta (2\theta+b+2-s) \right) \\ & - t_{s-1}^{\varpi-1} \mathscr{H}_1(t_{s-1}, \mathscr{X}^{s-1}, \mathscr{Y}^{s-1}, \mathscr{V}^{s-1}) \\ & \left. \times \left((-s+1+b)^{\theta+1} - (b-s)^\theta (-s+b+\theta+1) \right) \right] \\ \mathscr{Y}^{b+1} &= \mathscr{Y}^0 + \frac{\varpi(\Delta t)^\theta}{\Gamma(\theta+2)} \sum_{s=0}^{b} \left[t_{s-1}^{\varpi} \mathscr{H}_2(t_s, \mathscr{X}^s, \mathscr{Y}^s, \mathscr{V}^s) \right. \\ & \times \left((-s+b+1)^\theta (-s+\theta+b+2) - (b-s)^\theta (2\theta+b+2-s) \right) \\ & - t_{s-1}^{\varpi-1} \mathscr{H}_2(t_{s-1}, \mathscr{X}^{s-1}, \mathscr{Y}^{s-1}, \mathscr{V}^{s-1}) \\ & \left. \times \left((-s+1+b)^{\theta+1} - (b-s)^\theta (-s+b+\theta+1) \right) \right] \\ \mathscr{V}^{b+1} &= \mathscr{V}^0 + \frac{\varpi(\Delta t)^\theta}{\Gamma(\theta+2)} \sum_{s=0}^{b} \left[t_{s-1}^{\varpi} \mathscr{H}_3(t_s, \mathscr{X}^s, \mathscr{Y}^s, \mathscr{V}^s) \right. \\ & \times \left((-s+b+1)^\theta (-s+\theta+b+2) - (b-s)^\theta (2\theta+b+2-s) \right) \\ & - t_{s-1}^{\varpi-1} \mathscr{H}_3(t_{s-1}, \mathscr{X}^{s-1}, \mathscr{Y}^{s-1}, \mathscr{V}^{s-1}) \\ & \left. \times \left((-s+1+b)^{\theta+1} - (b-s)^\theta (-s+b+\theta+1) \right) \right] \end{cases} \tag{21}$$

5.2 Numerical scheme for Caputo-Fabrizio operator

Here, we present the numerical scheme of the model (1) under Caputo-Fabrizio-fractal-fractional derivative. Thus, the model (1) can be converted to the following

$$\begin{cases} {}^{\mathscr{CF}}\mathscr{D}_{0,t}^{\theta}(\mathscr{X}(t)) = \varpi t^{\varpi-1} \mathscr{H}_1(t, \mathscr{X}, \mathscr{Y}, \mathscr{V}), \\ {}^{\mathscr{CF}}\mathscr{D}_{0,t}^{\theta}(\mathscr{Y}(t)) = \varpi t^{\varpi-1} \mathscr{H}_2(t, \mathscr{X}, \mathscr{Y}, \mathscr{V}), \\ {}^{\mathscr{CF}}\mathscr{D}_{0,t}^{\theta}(\mathscr{V}(t)) = \varpi t^{\varpi-1} \mathscr{H}_3(t, \mathscr{X}, \mathscr{Y}, \mathscr{V}). \end{cases} \tag{22}$$

We apply the Caputo-Fabrizio integral to obtain the following integral equation

$$\begin{cases} \mathscr{X}(t) &= \mathscr{X}(0) + \frac{\varpi t^{\varpi-1}(1-\theta)}{\mathscr{M}(\theta)} \mathscr{H}_1(t, \mathscr{X}, \mathscr{Y}, \mathscr{V}) \\ & + \frac{\theta\varpi}{\mathscr{M}(\theta)} \int_0^t \psi^{\varpi-1} \mathscr{H}_1(t, \mathscr{X}, \mathscr{Y}, \mathscr{V}), \\ \mathscr{Y}(t) &= \mathscr{Y}(0) + \frac{\varpi t^{\varpi-1}(1-\theta)}{\mathscr{M}(\theta)} \mathscr{H}_2(t, \mathscr{X}, \mathscr{Y}, \mathscr{V}) \\ & + \frac{\theta\varpi}{\mathscr{M}(\theta)} \int_0^t \psi^{\varpi-1} \mathscr{H}_2(t, \mathscr{X}, \mathscr{Y}, \mathscr{V}), \\ \mathscr{V}(t) &= \mathscr{V}(0) + \frac{\varpi t^{\varpi-1}(1-\theta)}{\mathscr{M}(\theta)} \mathscr{H}_3(t, \mathscr{X}, \mathscr{Y}, \mathscr{V}) \\ & \frac{\theta\varpi}{\mathscr{M}(\theta)} \int_0^t \psi^{\varpi-1} \mathscr{H}_3(t, \mathscr{X}, \mathscr{Y}, \mathscr{V}). \end{cases} \tag{23}$$

Now, we present the derivation of the numerical scheme at $t = t_{b+1}$. Thus, we get

$$\begin{cases} \mathscr{X}^{b+1} &= \mathscr{X}^0 + \frac{\varpi t_b^{\varpi-1}(1-\theta)}{\mathscr{M}(\theta)} \mathscr{H}_1(t_b, \mathscr{X}^b, \mathscr{Y}^b, \mathscr{V}^b) \\ & + \frac{\theta\varpi}{\mathscr{M}(\theta)} \int_0^{t_{b+1}} \psi^{\varpi-1} \mathscr{H}_1(t, \mathscr{X}, \mathscr{Y}, \mathscr{V}) d\psi, \\ \mathscr{Y}^{b+1} &= \mathscr{Y}^0 + \frac{\varpi t_b^{\varpi-1}(1-\theta)}{\mathscr{M}(\theta)} \mathscr{H}_2(t_b, \mathscr{X}^b, \mathscr{Y}^b, \mathscr{V}^b) \\ & + \frac{\theta\varpi}{\mathscr{M}(\theta)} \int_0^{t_{b+1}} \psi^{\varpi-1} \mathscr{H}_2(t, \mathscr{X}, \mathscr{Y}, \mathscr{V}) d\psi, \\ \mathscr{V}^{b+1} &= \mathscr{V}^0 + \frac{\varpi t_b^{\varpi-1}(1-\theta)}{\mathscr{M}(\theta)} \mathscr{H}_3(t_b, \mathscr{X}^b, \mathscr{Y}^b, \mathscr{V}^b) \\ & \frac{\theta\varpi}{\mathscr{M}(\theta)} \int_0^{t_{b+1}} \psi^{\varpi-1} \mathscr{H}_3(t, \mathscr{X}, \mathscr{Y}, \mathscr{V}) d\psi. \end{cases} \tag{24}$$

Taking the difference between the consecutive terms, we get

$$\begin{cases} \mathscr{X}^{b+1} & = \mathscr{X}^{b} + \frac{\varpi t_b^{\varpi-1}(1-\theta)}{\mathscr{M}(\theta)}\mathscr{H}_1(t_b,\mathscr{X}^b,\mathscr{Y}^b,\mathscr{V}^b) \\ & -\frac{\varpi t_{b-1}^{\varpi-1}(1-\theta)}{\mathscr{M}(\theta)}\mathscr{H}_1(t_{b-1},\mathscr{X}^{b-1},\mathscr{Y}^{b-1},\mathscr{V}^{b-1}) \\ & +\frac{\theta\varpi}{\mathscr{M}(\theta)}\int_{t_b}^{t_{b+1}}\psi^{\varpi-1}\mathscr{H}_1(t,\mathscr{X},\mathscr{Y},\mathscr{V})d\psi, \\ \mathscr{Y}^{b+1} & = \mathscr{Y}^{b} + \frac{\varpi t_b^{\varpi-1}(1-\theta)}{\mathscr{M}(\theta)}\mathscr{H}_2(t_b,\mathscr{X}^b,\mathscr{Y}^b,\mathscr{V}^b) \\ & -\frac{\varpi t_{b-1}^{\varpi-1}(1-\theta)}{\mathscr{M}(\theta)}\mathscr{H}_2(t_{b-1},\mathscr{X}^{b-1},\mathscr{Y}^{b-1},\mathscr{V}^{b-1}) \\ & +\frac{\theta\varpi}{\mathscr{M}(\theta)}\int_{t_b}^{t_{b+1}}\psi^{\varpi-1}\mathscr{H}_2(t,\mathscr{X},\mathscr{Y},\mathscr{V})d\psi, \\ \mathscr{V}^{b+1} & = \mathscr{V}^{b} + \frac{\varpi t_b^{\varpi-1}(1-\theta)}{\mathscr{M}(\theta)}\mathscr{H}_3(t_b,\mathscr{X}^b,\mathscr{Y}^b,\mathscr{V}^b) \\ & -\frac{\varpi t_{b-1}^{\varpi-1}(1-\theta)}{\mathscr{M}(\theta)}\mathscr{H}_3(t_{b-1},\mathscr{X}^{b-1},\mathscr{Y}^{b-1},\mathscr{V}^{b-1}) \\ & +\frac{\theta\varpi}{\mathscr{M}(\theta)}\int_{t_b}^{t_{b+1}}\psi^{\varpi-1}\mathscr{H}_3(t,\mathscr{X},\mathscr{Y},\mathscr{V})d\psi, \end{cases} \tag{25}$$

Now, using integration and Lagrange polynomial interpolation, we get

$$\begin{cases} \mathscr{X}^{b+1} & = \mathscr{X}^{b} + \frac{\varpi t_b^{\varpi-1}(1-\theta)}{\mathscr{M}(\theta)}\mathscr{H}_1(t_b,\mathscr{X}^b,\mathscr{Y}^b,\mathscr{V}^b) \\ & -\frac{\varpi t_{b-1}^{\varpi-1}(1-\theta)}{\mathscr{M}(\theta)}\mathscr{H}_1(t_{b-1},\mathscr{X}^{b-1},\mathscr{Y}^{b-1},\mathscr{V}^{b-1}) + \frac{\theta\varpi}{\mathscr{M}(\theta)} \\ & \times\left[\frac{3}{2}(\Delta t)t_b^{\varpi-1}\mathscr{H}_1(t_b,\mathscr{X}^b,\mathscr{Y}^b,\mathscr{V}^b) - \frac{\Delta t}{2}t_{b-1}^{\varpi-1}\mathscr{H}_1(t_{b-1},\mathscr{X}^{b-1},\mathscr{Y}^{b-1},\mathscr{V}^{b-1})\right], \\ \mathscr{Y}^{b+1} & = \mathscr{Y}^{b} + \frac{\varpi t_b^{\varpi-1}(1-\theta)}{\mathscr{M}(\theta)}\mathscr{H}_2(t_b,\mathscr{X}^b,\mathscr{Y}^b,\mathscr{V}^b) \\ & -\frac{\varpi t_{b-1}^{\varpi-1}(1-\theta)}{\mathscr{M}(\theta)}\mathscr{H}_2(t_{b-1},\mathscr{X}^{b-1},\mathscr{Y}^{b-1},\mathscr{V}^{b-1}) + \frac{\theta\varpi}{\mathscr{M}(\theta)} \\ & \times\left[\frac{3}{2}(\Delta t)t_b^{\varpi-1}\mathscr{H}_1(t_b,\mathscr{X}^b,\mathscr{Y}^b,\mathscr{V}^b) - \frac{\Delta t}{2}t_{b-1}^{\varpi-1}\mathscr{H}_2(t_{b-1},\mathscr{X}^{b-1},\mathscr{Y}^{b-1},\mathscr{V}^{b-1})\right], \\ \mathscr{V}^{b+1} & = \mathscr{V}^{b} + \frac{\varpi t_b^{\varpi-1}(1-\theta)}{\mathscr{M}(\theta)}\mathscr{H}_3(t_b,\mathscr{X}^b,\mathscr{Y}^b,\mathscr{V}^b) \\ & -\frac{\varpi t_{b-1}^{\varpi-1}(1-\theta)}{\mathscr{M}(\theta)}\mathscr{H}_3(t_{b-1},\mathscr{X}^{b-1},\mathscr{Y}^{b-1},\mathscr{V}^{b-1}) + \frac{\theta\varpi}{\mathscr{M}(\theta)} \\ & \times\left[\frac{3}{2}(\Delta t)t_b^{\varpi-1}\mathscr{H}_3(t_b,\mathscr{X}^b,\mathscr{Y}^b,\mathscr{V}^b) - \frac{\Delta t}{2}t_{b-1}^{\varpi-1}\mathscr{H}_3(t_{b-1},\mathscr{X}^{b-1},\mathscr{Y}^{b-1},\mathscr{V}^{b-1})\right]. \end{cases} \tag{26}$$

5.3 Numerical scheme for Atangana-Baleanu operator

In this part, we consider the model (1) under AB fractal-fractional derivative as follows:

$$\begin{cases} {}^{\mathscr{AB}\mathscr{R}}\mathscr{D}_{0,t}^{\theta}(\mathscr{X}(t)) = \varpi t^{\varpi-1}\mathscr{H}_1(t,\mathscr{X},\mathscr{Y},\mathscr{V}), \\ {}^{\mathscr{AB}\mathscr{R}}\mathscr{D}_{0,t}^{\theta}(\mathscr{Y}(t)) = \varpi t^{\varpi-1}\mathscr{H}_2(t,\mathscr{X},\mathscr{Y},\mathscr{V}), \\ {}^{\mathscr{AB}\mathscr{R}}\mathscr{D}_{0,t}^{\theta}(\mathscr{V}(t)) = \varpi t^{\varpi-1}\mathscr{H}_3(t,\mathscr{X},\mathscr{Y},\mathscr{V}). \end{cases} \tag{27}$$

Continuing the above system to the AB in Caputo sense and implementing the corresponding AB fractional integral, we obtain

$$\begin{cases} \mathscr{X}(t) & = \mathscr{X}(0) + \frac{\varpi t^{\varpi-1}(1-\theta)}{\mathscr{AB}(\theta)}\mathscr{H}_1(t,\mathscr{X},\mathscr{Y},\mathscr{V}) \\ & +\frac{\theta\varpi}{\mathscr{AB}(\theta)\Gamma(\theta)}\int_0^t\psi^{\varpi-1}(t-\psi)^{\theta-1}\mathscr{H}_1(\psi,\mathscr{X},\mathscr{Y},\mathscr{V})d\psi, \\ \mathscr{Y}(t) & = \mathscr{Y}(0) + \frac{\varpi t^{\varpi-1}(1-\theta)}{\mathscr{AB}(\theta)}\mathscr{H}_2(t,\mathscr{X},\mathscr{Y},\mathscr{V}) \\ & +\frac{\theta\varpi}{\mathscr{AB}(\theta)\Gamma(\theta)}\int_0^t\psi^{\varpi-1}(t-\psi)^{\theta-1}\mathscr{H}_2(\psi,\mathscr{X},\mathscr{Y},\mathscr{V})d\psi, \\ \mathscr{V}(t) & = \mathscr{V}(0) + \frac{\varpi t^{\varpi-1}(1-\theta)}{\mathscr{AB}(\theta)}\mathscr{H}_3(t,\mathscr{X},\mathscr{Y},\mathscr{V}) \\ & +\frac{\theta\varpi}{\mathscr{AB}(\theta)\Gamma(\theta)}\int_0^t\psi^{\varpi-1}(t-\psi)^{\theta-1}\mathscr{H}_3(\psi,\mathscr{X},\mathscr{Y},\mathscr{V})d\psi \end{cases} \tag{28}$$

Now, at $t = t_{b+1}$, we get

$$\begin{cases} \mathscr{X}^{b+1} & = \mathscr{X}^0 + \frac{\varpi t_b^{\varpi-1}(1-\theta)}{\mathscr{AB}(\theta)}\mathscr{H}_1(t_b,\mathscr{X}^b,\mathscr{Y}^b,\mathscr{V}^b) \\ & + \frac{\theta\varpi}{\mathscr{AB}(\theta)\Gamma(\theta)}\int_0^{t_{b+1}}\psi^{\varpi-1}(t_{b+1}-\psi)^{\theta-1}\mathscr{H}_1(\psi,\mathscr{X},\mathscr{Y},\mathscr{V})d\psi, \\ \mathscr{Y}^{b+1} & = \mathscr{Y}^0 + \frac{\varpi t_b^{\varpi-1}(1-\theta)}{\mathscr{AB}(\theta)}\mathscr{H}_2(t_b,\mathscr{X}^b,\mathscr{Y}^b,\mathscr{V}^b) \\ & + \frac{\theta\varpi}{\mathscr{AB}(\theta)\Gamma(\theta)}\int_0^{t_{b+1}}\psi^{\varpi-1}(t_{b+1}-\psi)^{\theta-1}\mathscr{H}_2(\psi,\mathscr{X},\mathscr{Y},\mathscr{V})d\psi, \\ \mathscr{V}^{b+1} & = \mathscr{V}^0 + \frac{\varpi t_n^{\varpi-1}(1-\theta)}{\mathscr{AB}(\theta)}\mathscr{H}_3(t_n,\mathscr{X}^n,\mathscr{Y}^n,\mathscr{V}^n) \\ & + \frac{\theta\varpi}{\mathscr{AB}(\theta)\Gamma(\theta)}\int_0^{t_{b+1}}\psi^{\varpi-1}(t_{b+1}-\psi)^{\theta-1}\mathscr{H}_3(\psi,\mathscr{X},\mathscr{Y},\mathscr{V})d\psi. \end{cases} \tag{29}$$

Using the approximation of the integrals on the right hand side of system (29), we achieve

$$\begin{cases} \mathscr{X}^{b+1} & = \mathscr{X}^0 + \frac{\varpi t_b^{\varpi-1}(1-\theta)}{\mathscr{AB}(\theta)}\mathscr{H}_1(t_b,\mathscr{X}^b,\mathscr{Y}^b,\mathscr{V}^b) \\ & + \frac{\theta\varpi}{\mathscr{AB}(\theta)\Gamma(\theta)}\sum_{s=0}^{b}\int_{t_s}^{t_{s+1}}\psi^{\varpi-1}(t_{b+1}-\psi)^{\theta-1}\mathscr{H}_1(\psi,\mathscr{X},\mathscr{Y},\mathscr{V})d\psi, \\ \mathscr{Y}^{b+1} & = \mathscr{Y}^0 + \frac{\varpi t_b^{\varpi-1}(1-\theta)}{\mathscr{AB}(\theta)}\mathscr{H}_2(t_b,\mathscr{X}^b,\mathscr{Y}^b,\mathscr{V}^b) \\ & + \frac{\theta\varpi}{\mathscr{AB}(\theta)\Gamma(\theta)}\sum_{s=0}^{b}\int_{t_s}^{t_{s+1}}\psi^{\varpi-1}(t_{b+1}-\psi)^{\theta-1}\mathscr{H}_2(\psi,\mathscr{X},\mathscr{Y},\mathscr{V})d\psi, \\ \mathscr{V}^{b+1} & = \mathscr{V}^0 + \frac{\varpi t_b^{\varpi-1}(1-\theta)}{\mathscr{AB}(\theta)}\mathscr{H}_3(t_b,\mathscr{X}^b,\mathscr{Y}^b,\mathscr{V}^b) \\ & + \frac{\theta\varpi}{\mathscr{AB}(\theta)\Gamma(\theta)}\sum_{s=0}^{b}\int_{t_s}^{t_{s+1}}\psi^{\varpi-1}(t_{b+1}-\psi)^{\theta-1}\mathscr{H}_3(\psi,\mathscr{X},\mathscr{Y},\mathscr{V})d\psi. \end{cases} \tag{30}$$

Now, with the aid of Lagrangian polynomial piece-wise interpolation, we achieve the general relation as follows:

$$\begin{cases} \mathscr{X}^{b+1} & = \mathscr{X}^0 + \frac{\varpi t_b^{\varpi-1}(1-\theta)}{\mathscr{AB}(\theta)}\mathscr{H}_1(t_b,\mathscr{X}^b,\mathscr{Y}^b,\mathscr{V}^b) + \frac{\varpi(\Delta t)^\theta}{\mathscr{AB}(\theta)\Gamma(\theta+2)} \\ & \times\sum_{s=0}^{b}\left[t_s^{\varpi-1}\mathscr{H}_1(t_s,\mathscr{X}^s,\mathscr{Y}^s,\mathscr{V}^s)\right. \\ & \times\left((-s+b+1)^\theta(\theta+2-s+b)-(b-s)^\theta(-s+b+2\theta+2)\right) \\ & -t_{s-1}^{\varpi-1}\mathscr{H}_1(t_{s-1},\mathscr{X}^{s-1},\mathscr{Y}^{s-1},\mathscr{V}^{s-1}) \\ & \left.\times\left((-s+1+b)^{\theta+1}-(b-s)^\theta(1+\theta-s+b)\right)\right], \\ \mathscr{Y}^{b+1} & = \mathscr{Y}^0 + \frac{\varpi t_b^{\varpi-1}(1-\theta)}{\mathscr{AB}(\theta)}\mathscr{H}_2(t_b,\mathscr{X}^b,\mathscr{Y}^b,\mathscr{V}^b) + \frac{\varpi(\Delta t)^\theta}{\mathscr{AB}(\theta)\Gamma(\theta+2)} \\ & \times\sum_{s=0}^{b}\left[t_s^{\varpi-1}\mathscr{H}_2(t_s,\mathscr{X}^s,\mathscr{Y}^s,\mathscr{V}^s)\right. \\ & \times\left((-s+b+1)^\theta(\theta+2-s+b)-(b-s)^\theta(-s+b+2\theta+2)\right) \\ & -t_{s-1}^{\varpi-1}\mathscr{H}_2(t_{s-1},\mathscr{X}^{s-1},\mathscr{Y}^{s-1},\mathscr{V}^{s-1}) \\ & \left.\times\left((-s+1+b)^{\theta+1}-(b-s)^\theta(1+\theta-s+b)\right)\right], \\ \mathscr{V}^{b+1} & = \mathscr{V}^0 + \frac{\varpi t_b^{\varpi-1}(1-\theta)}{\mathscr{AB}(\theta)}\mathscr{H}_3(t_b,\mathscr{X}^b,\mathscr{Y}^b,\mathscr{V}^b) + \frac{\varpi(\Delta t)^\theta}{\mathscr{AB}(\theta)\Gamma(\theta+2)} \\ & \times\sum_{s=0}^{b}\left[t_s^{\varpi-1}\mathscr{H}_3(t_s,\mathscr{X}^s,\mathscr{Y}^s,\mathscr{V}^s)\right. \\ & \times\left((-s+b+1)^\theta(\theta+2-s+b)-(b-s)^\theta(-s+b+2\theta+2)\right) \\ & -t_{s-1}^{\varpi-1}\mathscr{H}_3(t_{s-1},\mathscr{X}^{s-1},\mathscr{Y}^{s-1},\mathscr{V}^{s-1}) \\ & \left.\times\left((-s+1+b)^{\theta+1}-(b-s)^\theta(1+\theta-s+b)\right)\right], \end{cases} \tag{31}$$

Table 1: Parametric and initial values for simulations

Parameters	values	units
$\mathscr{X}(0)$	1.7×10^8	$\frac{\text{cell}}{\text{mL}}$
$\mathscr{Y}(0)$	0	$\frac{\text{cell}}{\text{mL}}$
$\mathscr{V}(0)$	400	$\frac{\text{copies}}{\text{mL}}$
λ^*	0.5	$\frac{\text{cell}}{\text{mL.day}}$
μ^*	0.5	day^{-1}
ρ	2.04	$\frac{\text{mL.}}{\text{copies.day}}$
ϑ	0.1	day^{-1}
c^*	6.24	day^{-1}
κ	0.65	day^{-1}
γ^*	0.65	day^{-1}

6 Numerical simulations

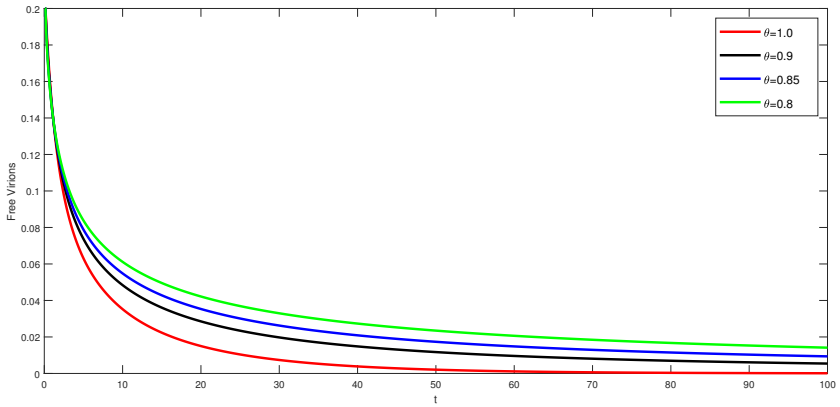

Fig. 1: Dynamical behavior of $\mathscr{V}(t)$ at ϖ=0.98 and various fractional order under power law kernel.

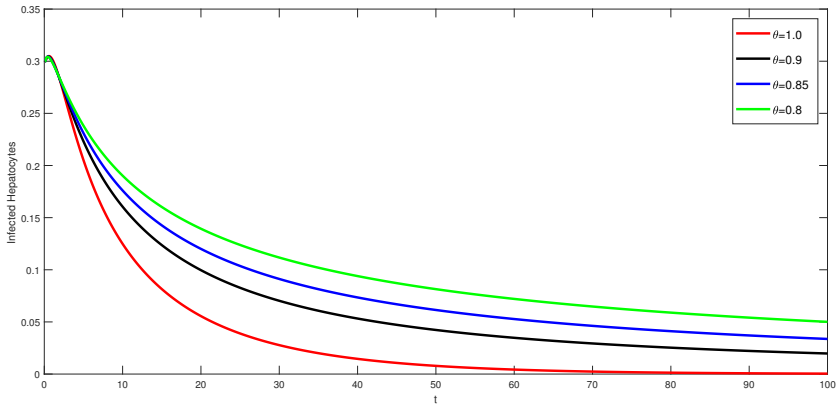

Fig. 2: Dynamical behavior of $\mathscr{Y}(t)$ at ϖ=0.98 and various fractional order under power law kernel.

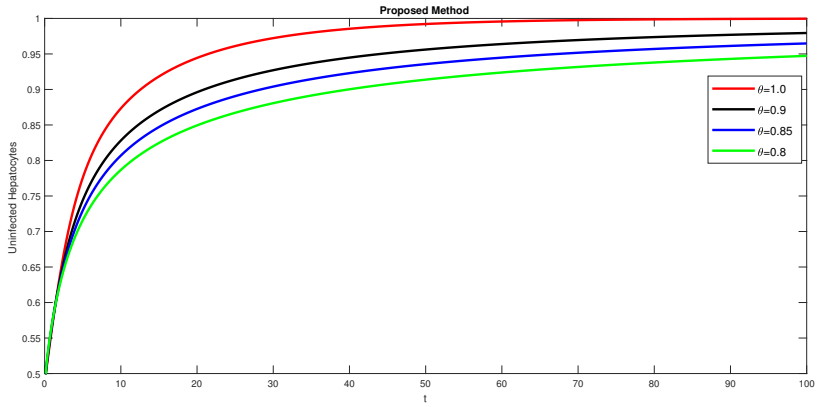

Fig. 3: Dynamical behavior of $\mathscr{X}(t)$ at ϖ=0.98 and various fractional order under power law kernel.

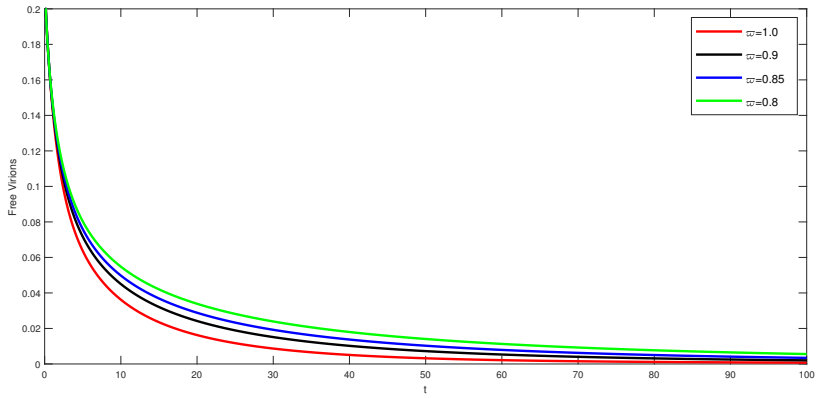

Fig. 4: Dynamical behavior of $\mathscr{V}(t)$ at θ=0.98 and various fractal order under power law kernel.

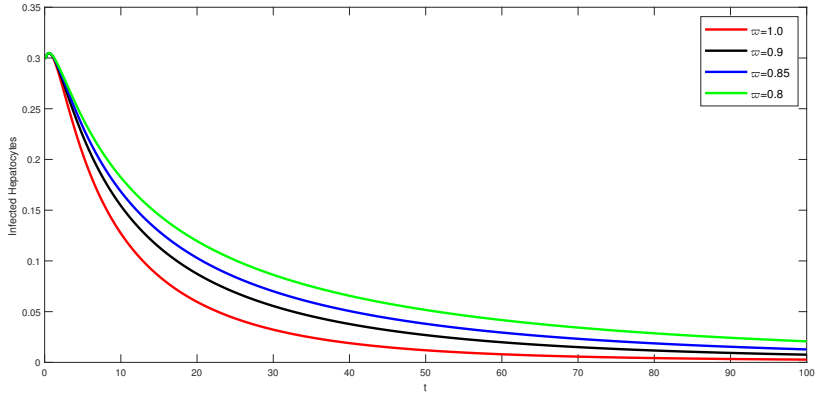

Fig. 5: Dynamical behavior of $\mathscr{Y}(t)$ at θ=0.98 and various fractal order under power law kernel.

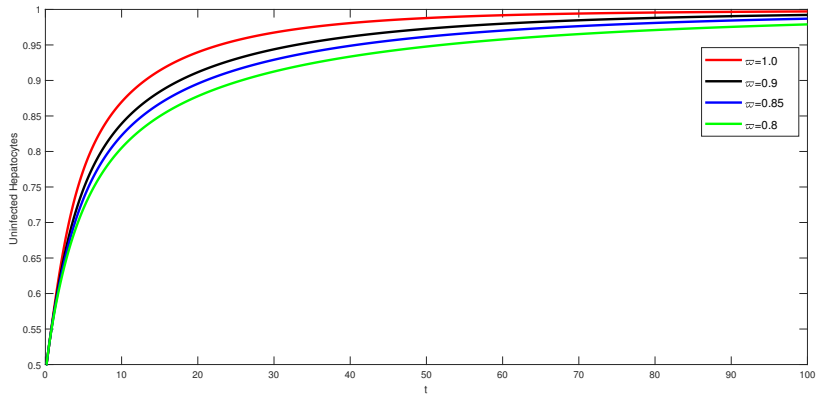

Fig. 6: Dynamical behavior of $\mathscr{X}(t)$ at θ=0.98 and various fractal order under power law kernel.

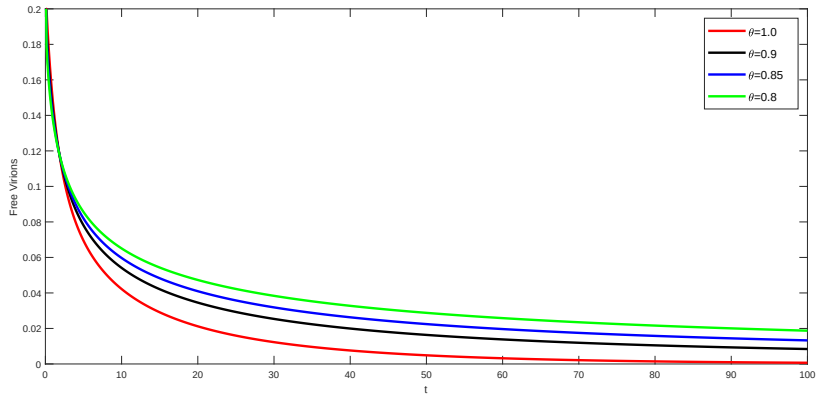

Fig. 7: Dynamical behavior of $\mathscr{V}(t)$ at ϖ=0.9 and various fractional order under power law kernel.

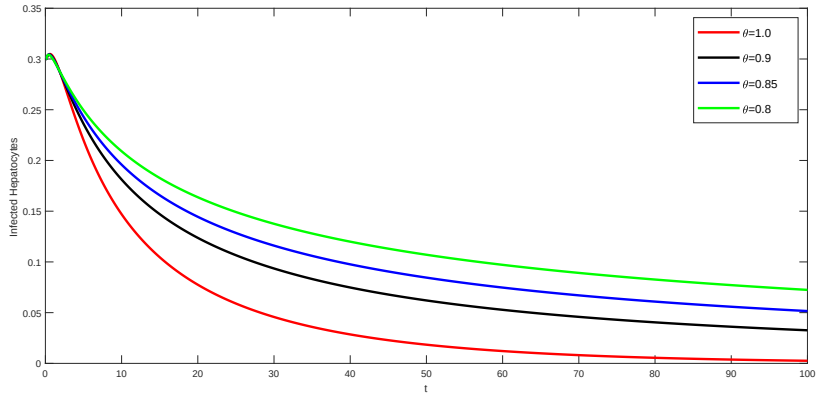

Fig. 8: Dynamical behavior of $\mathscr{Y}(t)$ at ϖ=0.9 and various fractional order under power law kernel.

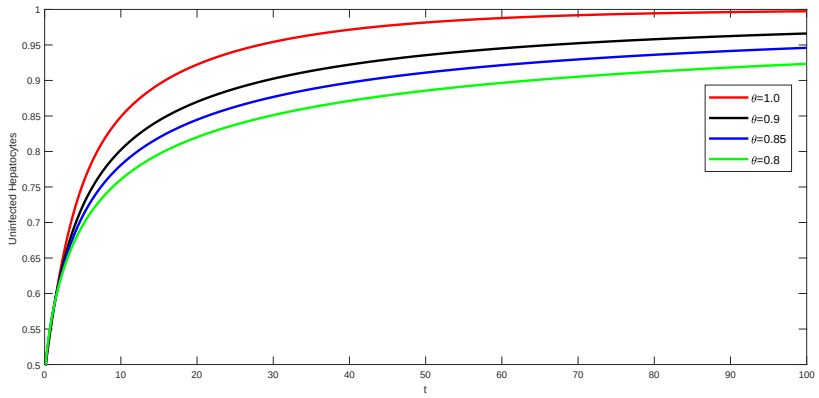

Fig. 9: Dynamical behavior of $\mathscr{X}(t)$ at ϖ=0.9 and various fractional order under power law kernel.

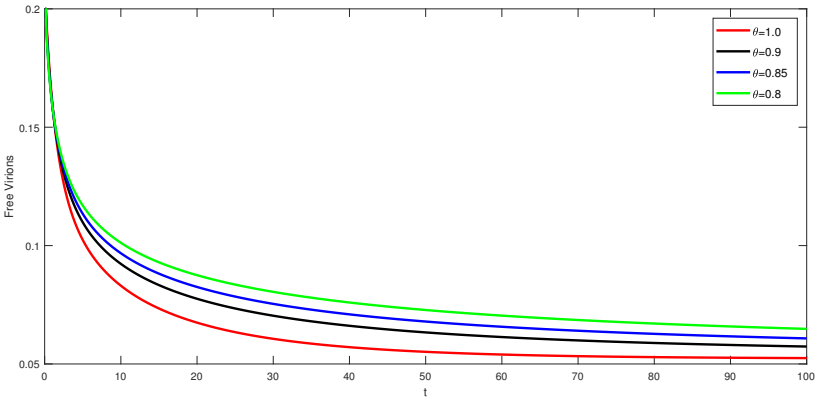

Fig. 10: Dynamical behavior of $\mathscr{V}(t)$ at ϖ=0.98 and various fractional order under power law kernel.

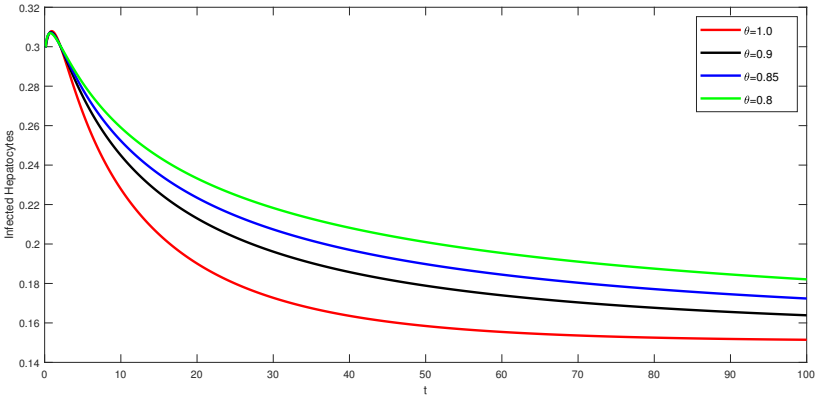

Fig. 11: Dynamical behavior of $\mathscr{Y}(t)$ at ϖ=0.98 and various fractional order under power law kernel.

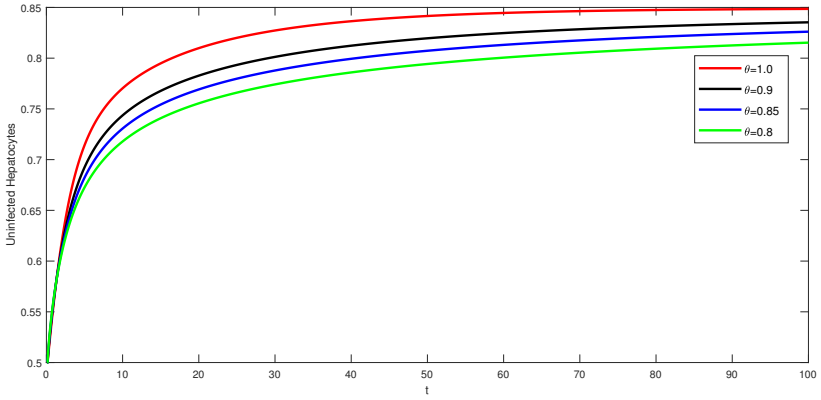

Fig. 12: Dynamical behavior of $\mathscr{X}(t)$ at ϖ=0.98 and various fractional order under power law kernel.

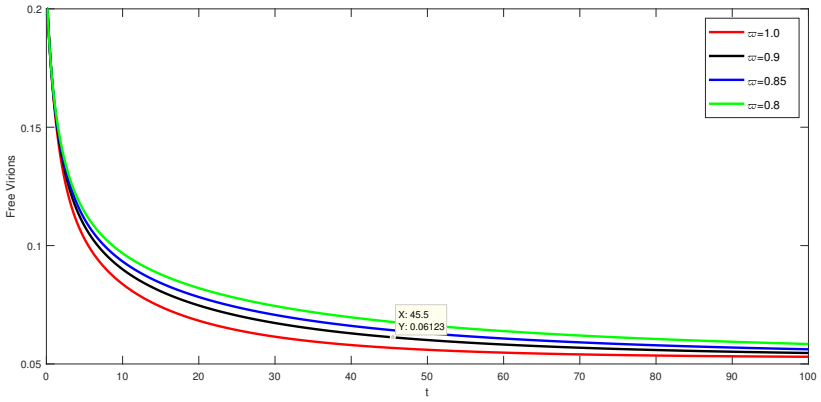

Fig. 13: Dynamical behavior of $\mathscr{V}(t)$ at θ=0.98 and various fractal order under power law kernel.

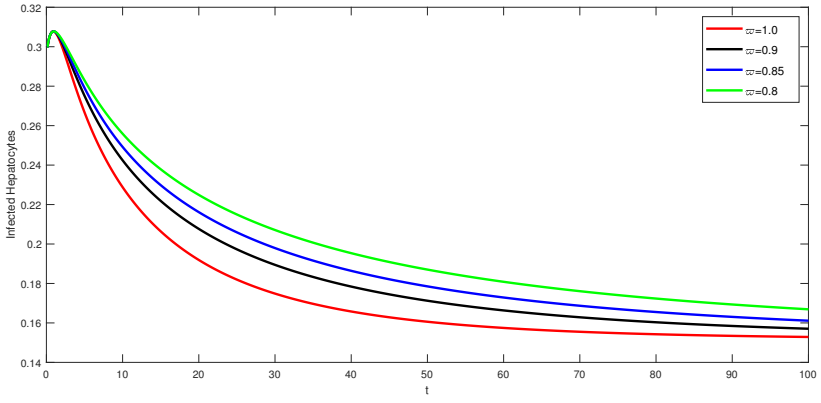

Fig. 14: Dynamical behavior of $\mathscr{Y}(t)$ at θ=0.98 and various fractal order under power law kernel.

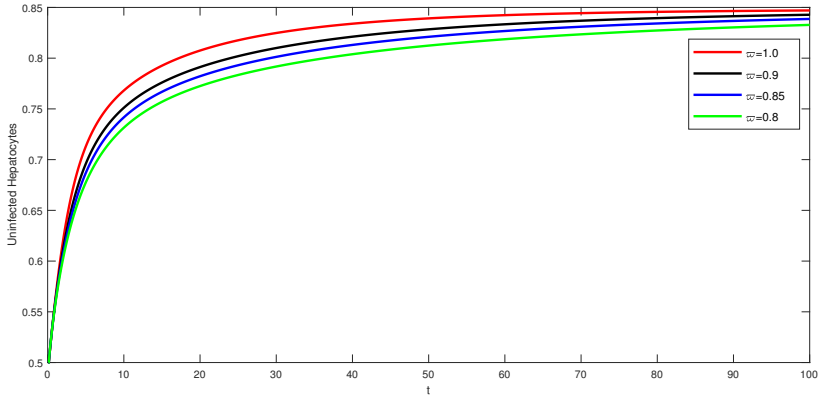

Fig. 15: Dynamical behavior of $\mathscr{X}(t)$ at θ=0.98 and various fractal order under power law kernel.

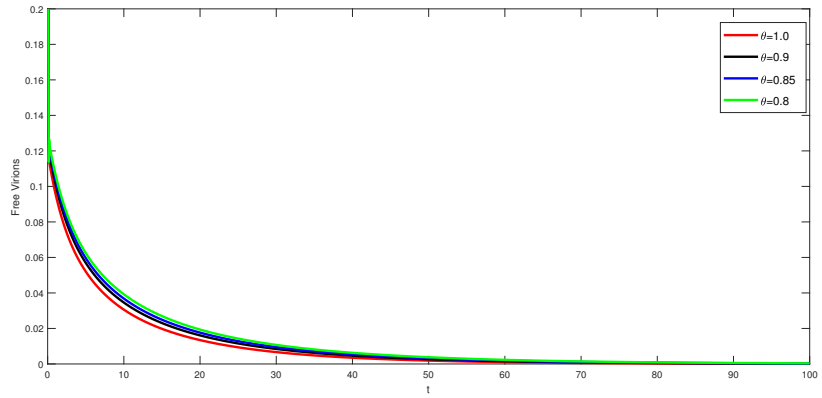

Fig. 16: Dynamical behavior of $\mathscr{V}(t)$ at ϖ=0.98 and various fractional order under exponential decay kernel.

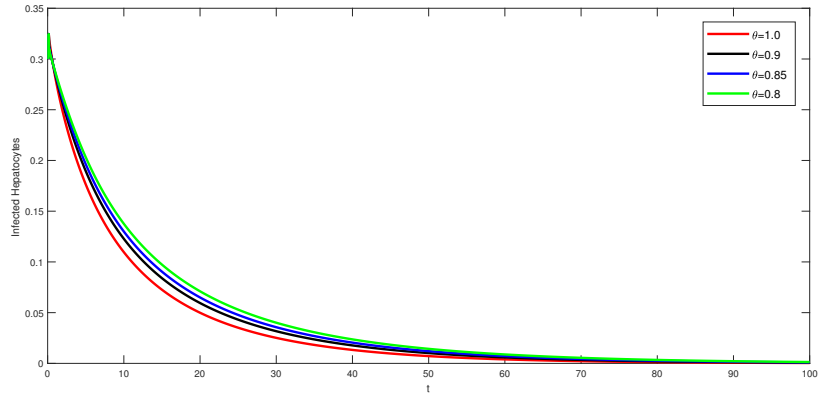

Fig. 17: Dynamical behavior of $\mathscr{Y}(t)$ at ϖ=0.98 and various fractional order under exponential decay kernel.

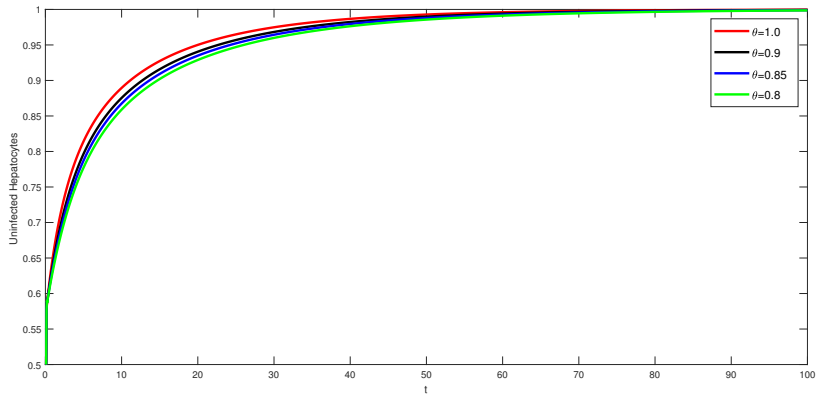

Fig. 18: Dynamical behavior of $\mathscr{X}(t)$ at ϖ=0.98 and various fractional order under exponential decay kernel.

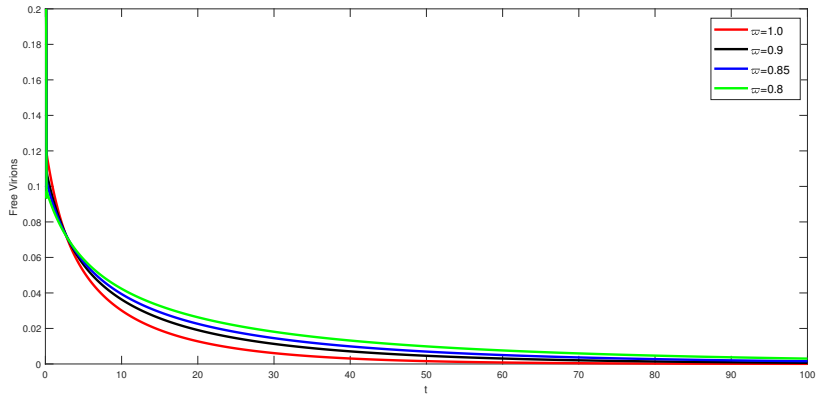

Fig. 19: Dynamical behavior of $\mathscr{V}(t)$ at θ=0.98 and various fractal order under exponential decay kernel.

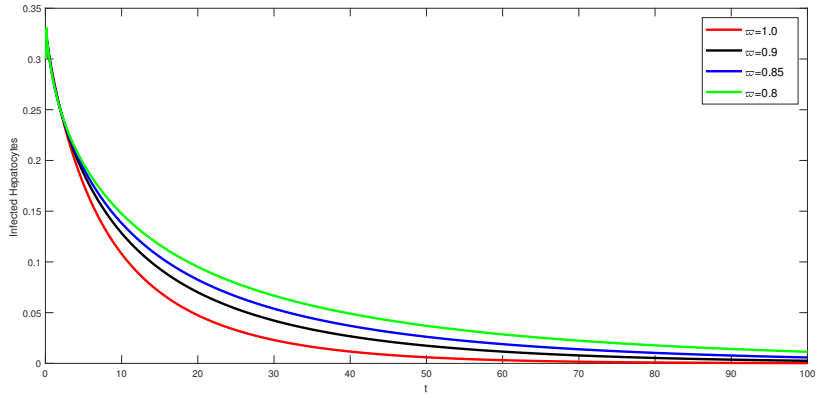

Fig. 20: Dynamical behavior of $\mathscr{Y}(t)$ at θ=0.98 and various fractal order under exponential decay kernel.

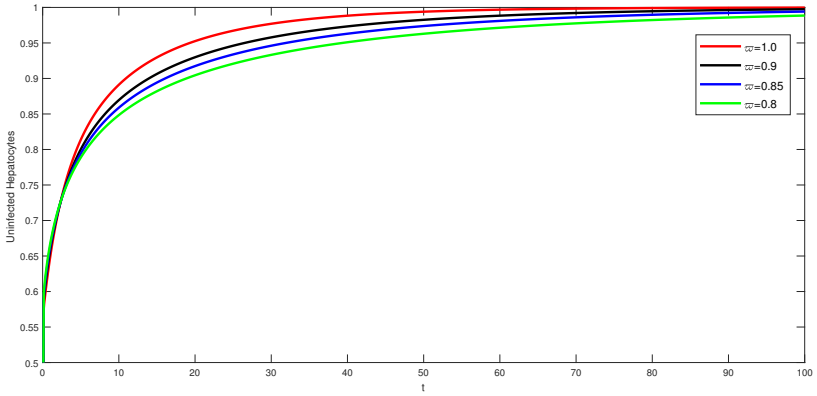

Fig. 21: Dynamical behavior of $\mathscr{X}(t)$ at θ=0.98 and various fractal order under exponential decay kernel.

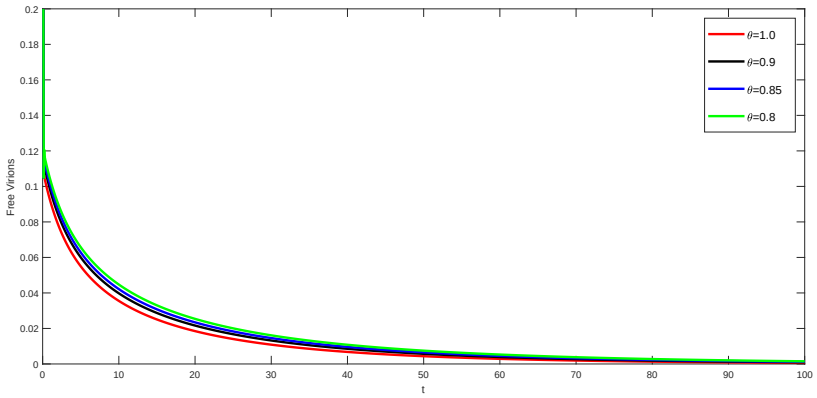

Fig. 22: Dynamical behavior of $\mathscr{V}(t)$ at ϖ=0.9 and various fractional order under exponential decay kernel.

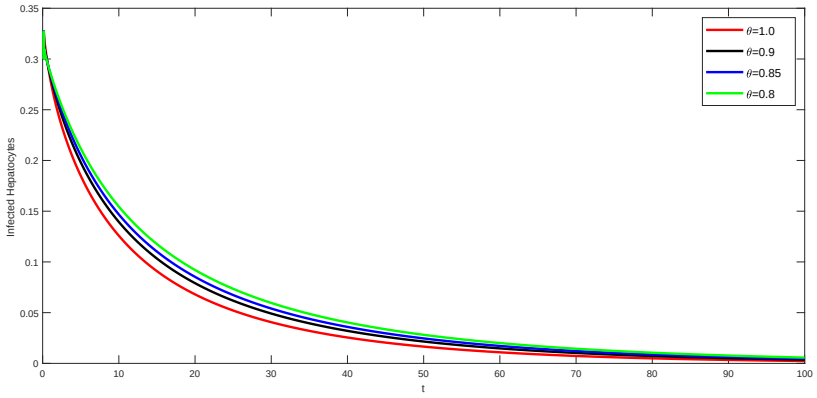

Fig. 23: Dynamical behavior of $\mathscr{Y}(t)$ at ϖ=0.9 and various fractional order under exponential decay kernel.

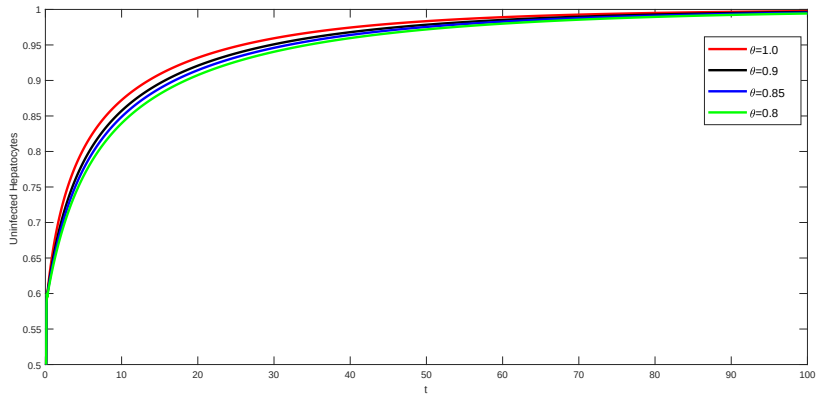

Fig. 24: Dynamical behavior of $\mathscr{X}(t)$ at ϖ=0.9 and various fractional order under exponential decay kernel.

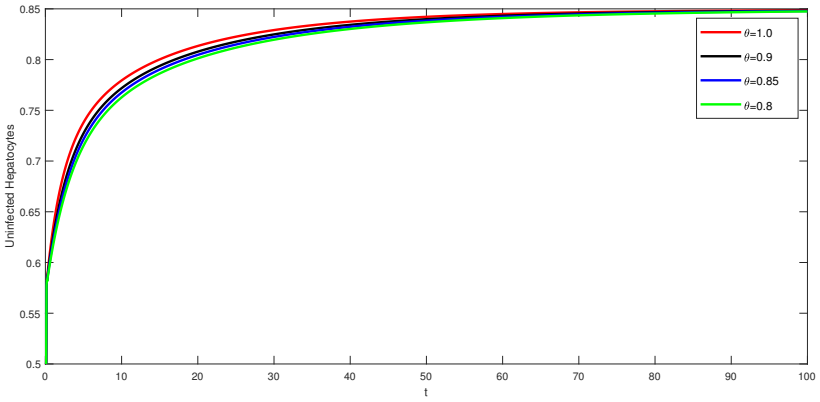

Fig. 25: Dynamical behavior of $\mathscr{V}(t)$ at ϖ=0.98 and various fractional order under power law kernel.

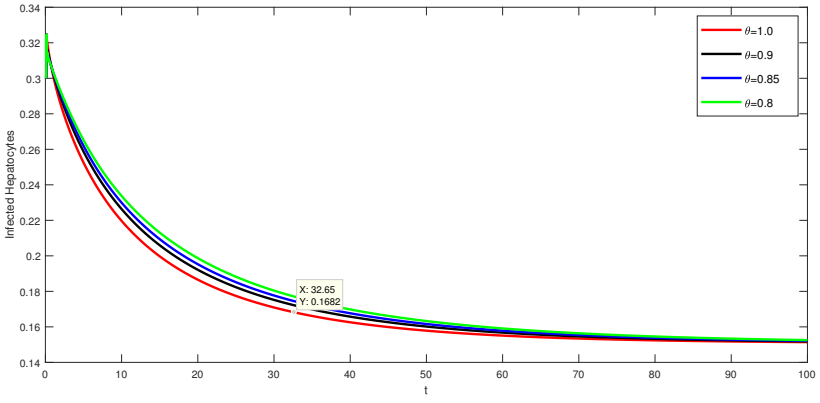

Fig. 26: Dynamical behavior of $\mathscr{Y}(t)$ at ϖ=0.98 and various fractional order under power law kernel.

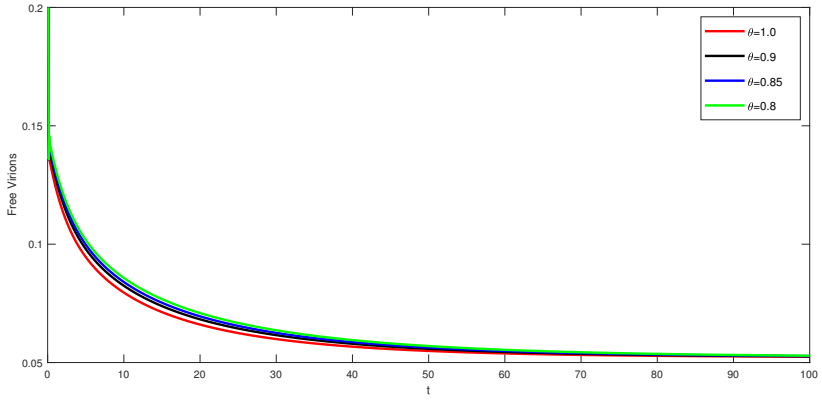

Fig. 27: Dynamical behavior of $\mathscr{X}(t)$ at ϖ=0.98 and various fractional order under power law kernel.

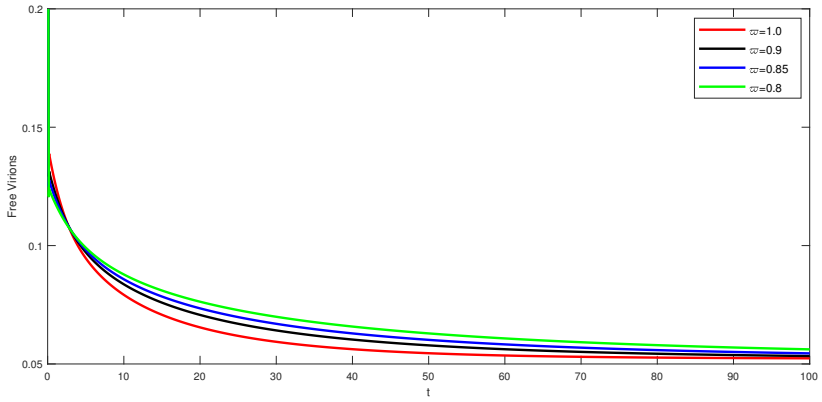

Fig. 28: Dynamical behavior of $\mathscr{V}(t)$ at θ=0.98 and various fractal order under power law kernel.

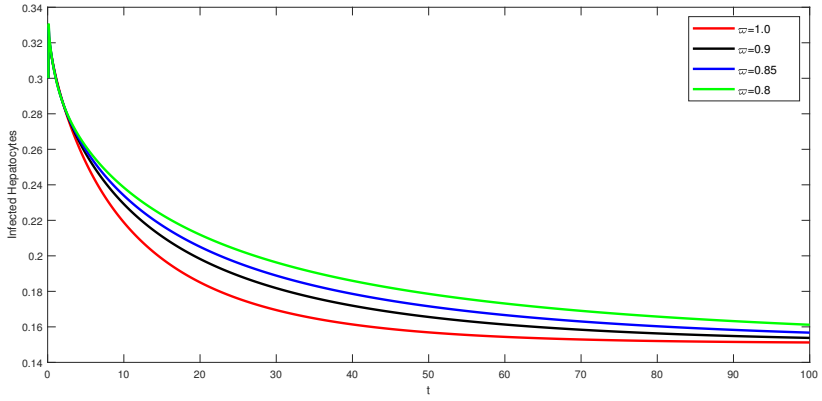

Fig. 29: Dynamical behavior of $\mathscr{Y}(t)$ at θ=0.98 and various fractal order under power law kernel.

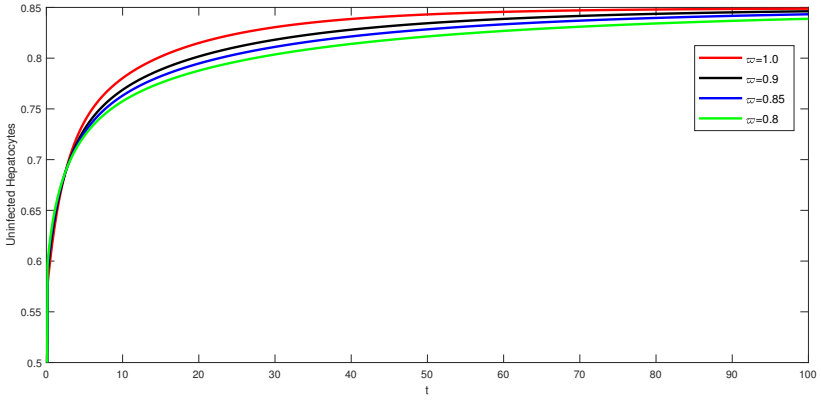

Fig. 30: Dynamical behavior of $\mathscr{X}(t)$ at θ=0.98 and various fractal order under power law kernel.

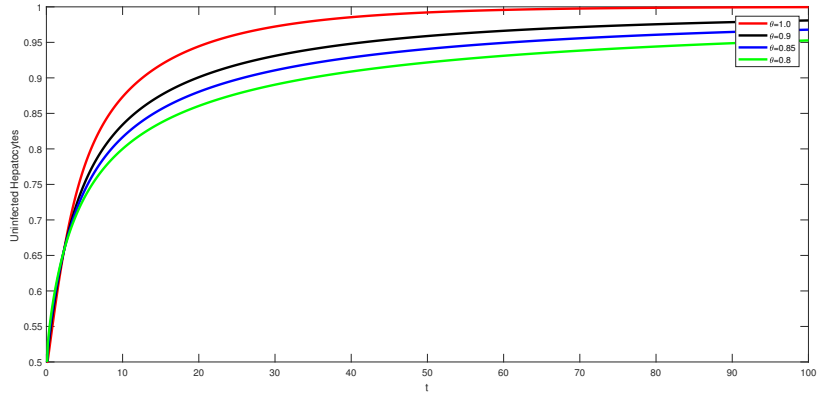

Fig. 31: Dynamical behavior of $\mathscr{V}(t)$ at ϖ=0.98 and various fractional order under Mittag-Leffler kernel.

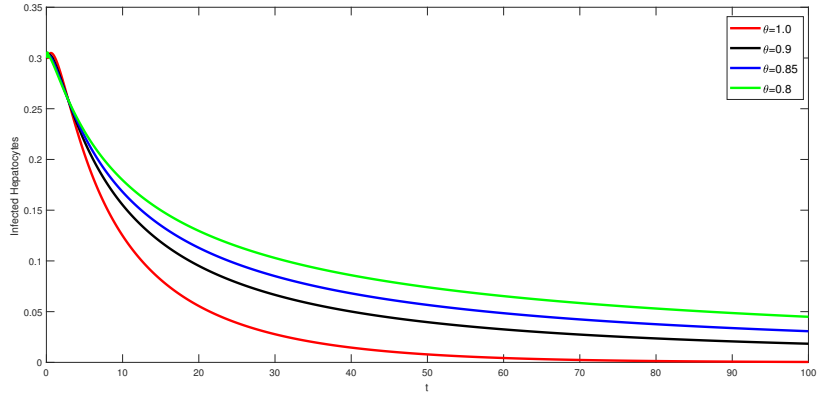

Fig. 32: Dynamical behavior of $\mathscr{Y}(t)$ at ϖ=0.98 and various fractional order under Mittag-Leffler kernel.

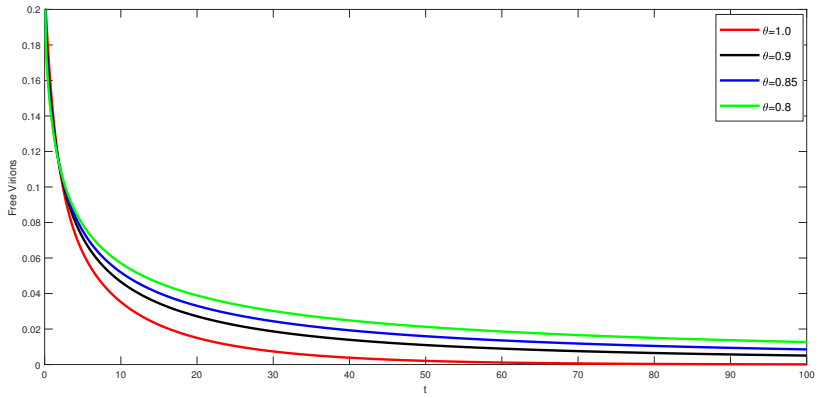

Fig. 33: Dynamical behavior of $\mathscr{X}(t)$ at ϖ=0.98 and various fractional order under Mittag-Leffler kernel.

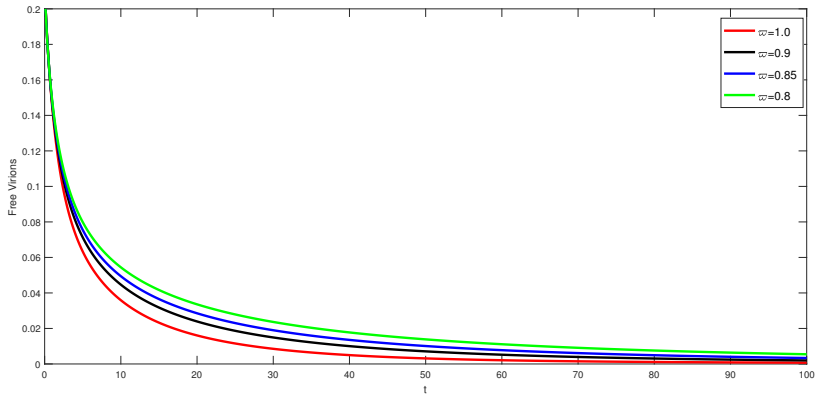

Fig. 34: Dynamical behavior of $\mathscr{V}(t)$ at θ=0.98 and various fractal order under Mittag-Leffler kernel.

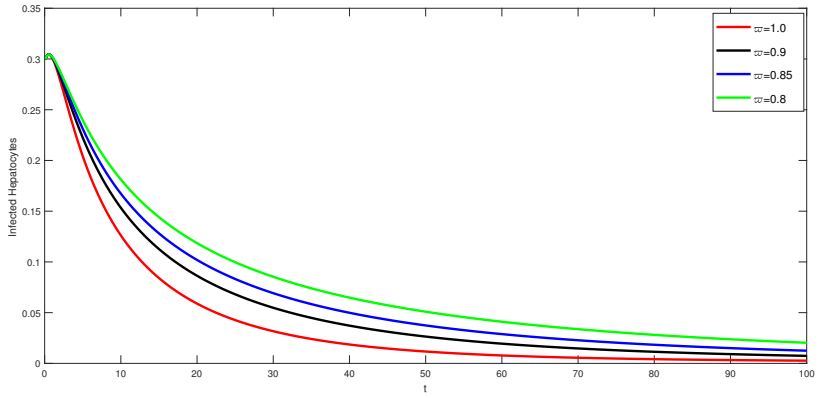

Fig. 35: Dynamical behavior of $\mathscr{Y}(t)$ at θ=0.98 and various fractal order under Mittag-Leffler kernel.

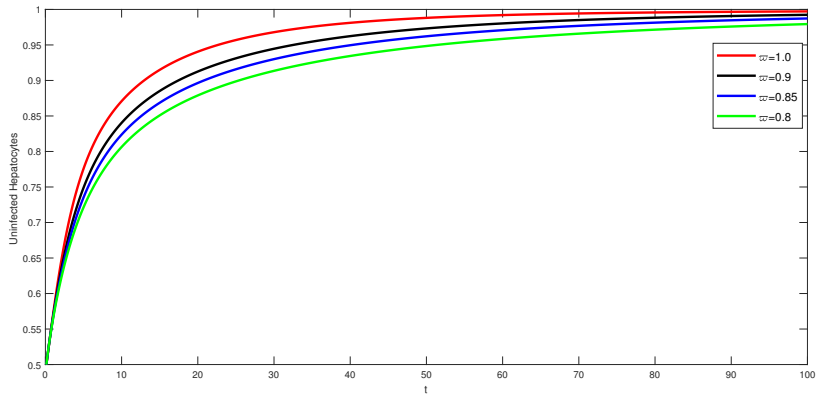

Fig. 36: Dynamical behavior of $\mathscr{X}(t)$ at θ=0.98 and various fractal order under Mittag-Leffler kernel.

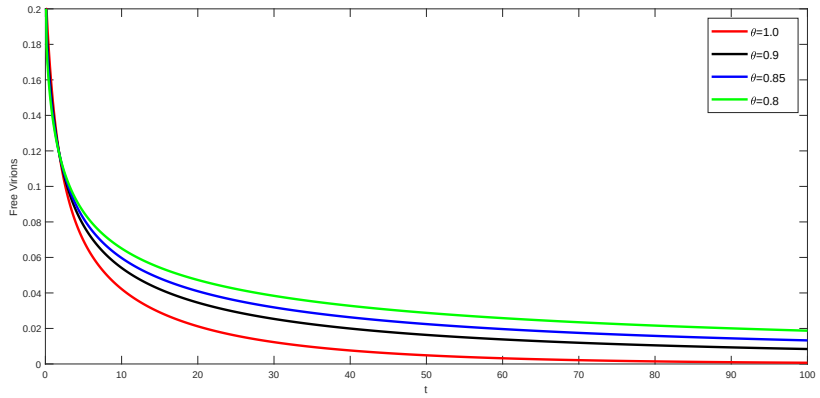

Fig. 37: Dynamical behavior of $\mathscr{V}(t)$ at ϖ=0.9 and various fractional order under Mittag-Leffler kernel.

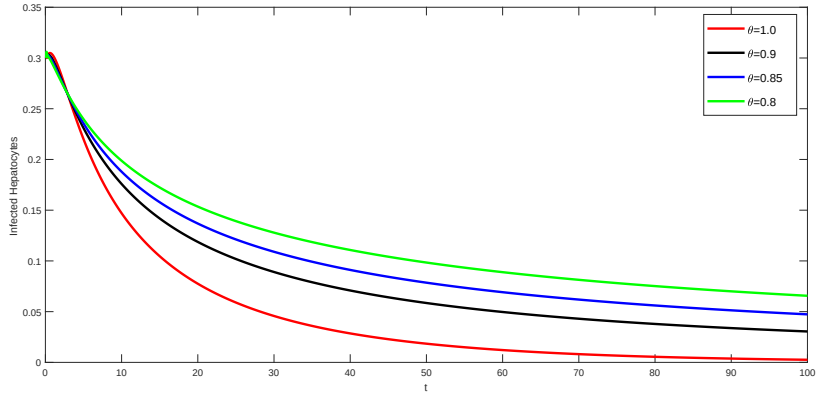

Fig. 38: Dynamical behavior of $\mathscr{Y}(t)$ at ϖ=0.9 and various fractional order under Mittag-Leffler kernel.

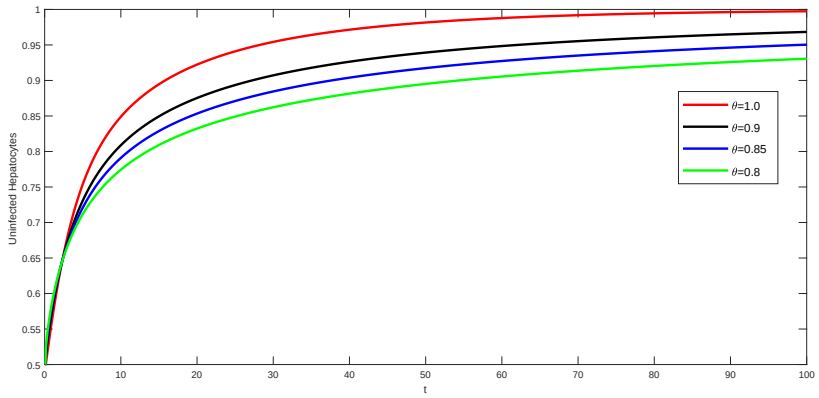

Fig. 39: Dynamical behavior of $\mathscr{X}(t)$ at ϖ=0.9 and various fractional order under Mittag-Leffler kernel.

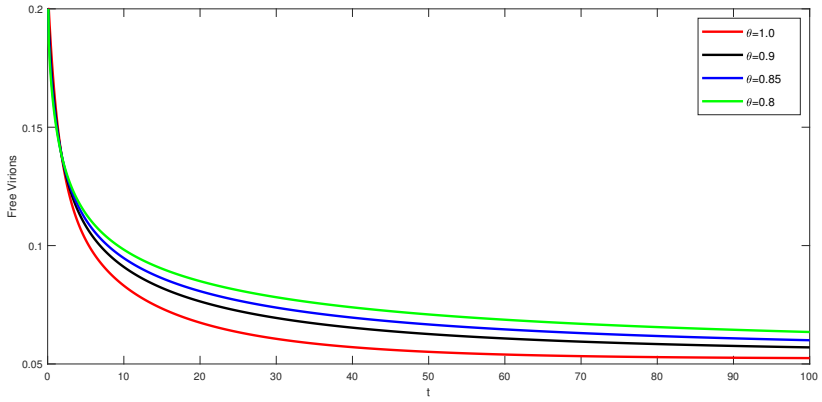

Fig. 40: Dynamical behavior of $\mathscr{V}(t)$ at ϖ=0.98 and various fractional order under power law kernel.

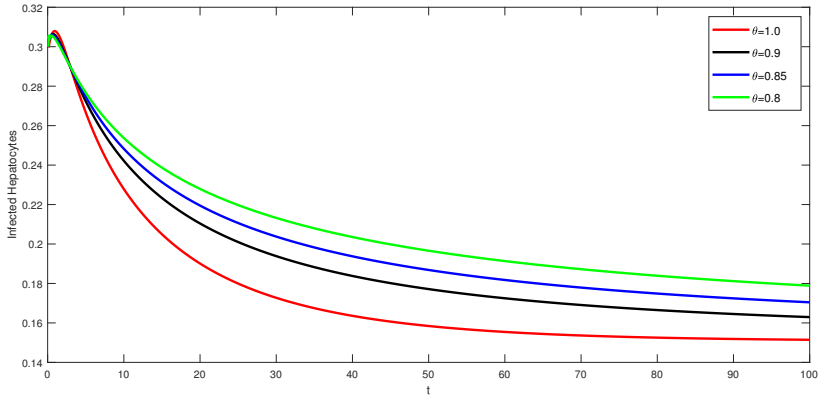

Fig. 41: Dynamical behavior of $\mathscr{Y}(t)$ at ϖ=0.98 and various fractional order under power law kernel.

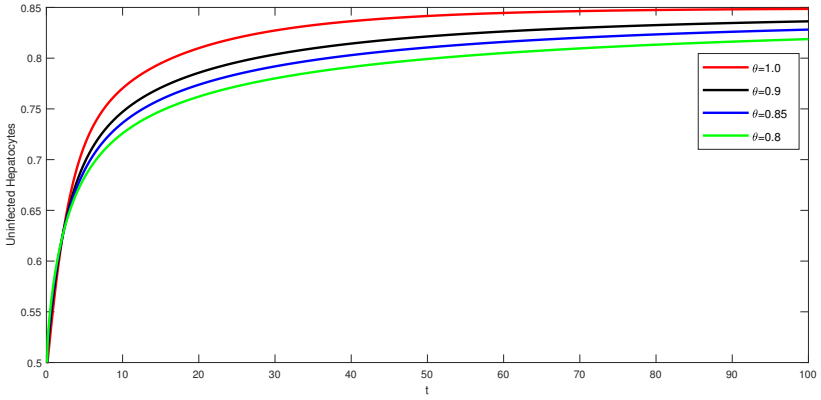

Fig. 42: Dynamical behavior of $\mathscr{X}(t)$ at ϖ=0.98 and various fractional order under power law kernel.

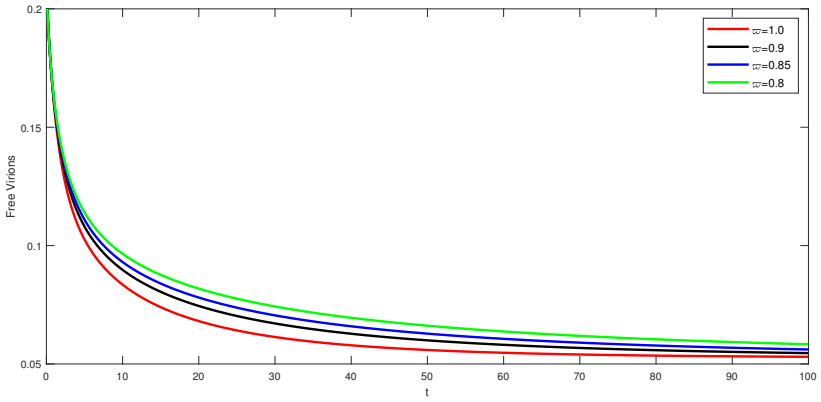

Fig. 43: Dynamical behavior of $\mathscr{V}(t)$ at θ=0.98 and various fractal order under power law kernel.

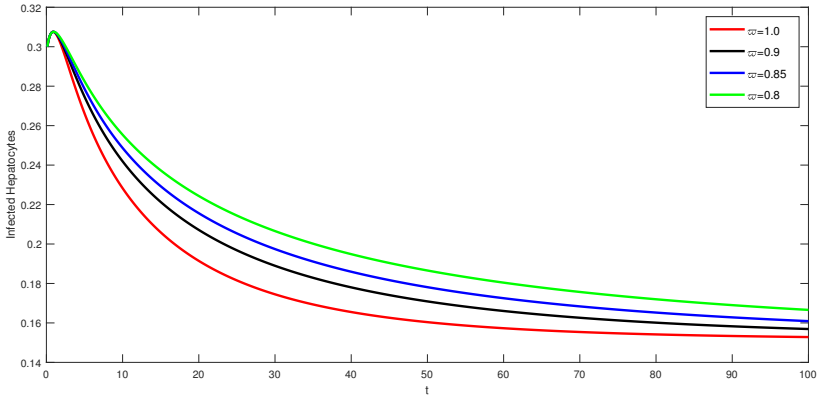

Fig. 44: Dynamical behavior of $\mathscr{Y}(t)$ at θ=0.98 and various fractal order under power law kernel.

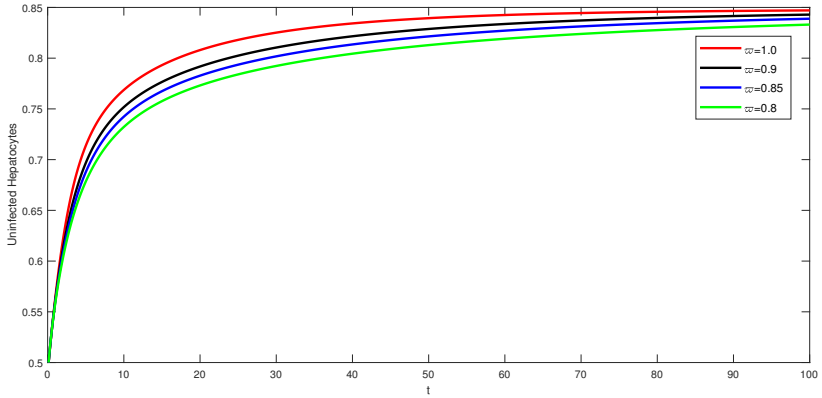

Fig. 45: Dynamical behavior of $\mathscr{X}(t)$ at θ=0.98 and various fractal order under power law kernel.

This section aims to simulate the numerical solutions of the model 8 under different fractal fractional operators and for different delay values. The values of parameters and initial conditions which have used for numerical simulations are given in Table 1. The graphic results are obtained for a different set of fractional and fractal order values and τ equals to 0.7 and 0.1, suggesting that novel operators have useful infection reduction results. The graphical representations are obtained at various values of fractal and fractional orders and delay term τ = 0.7 for the Caputo in Figures 1 to Figure 9, Caputo-Fabrizio in Figure 16 to Figure 24 and Atangana-Baleanu in Figure 31 to Figure 39. For τ = 0.1, Figure 10 to Figure 15, Figure 25 to Figure 30, Figure 40 to Figure 45, represents the dynamics of the proposed model for Caputo, Caputo-Fabrizio and Atangana-Baleanu operators. In all figures, the uninfected hepatocyte population increases as the population of infected hepatocytes and free virions reduce as time increases. We also note the effect of the delay term, for τ=0.1, as the fractional or fractal order increases, the free virions gradually decreases, but for $\tau = 0.7$ the free virions increase rapidly. These behaviour are due to the increase and decrease of fractional or fractal orders. As fractional-order operators provide a complete spectrum of dynamics, therefore we have taken only few order for analysis. As we see that increasing the fractional or fractal order, the faster decay and growth process. Also, we analyze the effect of fractional and fractal orders on each other by varying the order of θ and kept ϖ fix or changing values of ϖ and kept θ constant. The stability of the model has also observed due to the variation of the ϖ and θ. When ϖ=1, then the curves of the model converges to the fractional-order model. When both ϖ and θ equal to 1, the proposed model converges to the integer-order model. Thus fractal-fractional operators provide a global dynamics of a physical model [28]-[36].

7 Conclusion

In this paper, the hepatitis B virus with immune delay is proposed under the newly proposed operators called fractal-fractional operators. The basic reproduction number and equilibrium points of the model are calculated. The stability of equilibrium points is derived through the concept of Routh Hurtwez criterion. The existence and uniqueness theorems are proved through fixed point theory and guarantee that the model posses at least one solution and a unique solution. The notion of Ulam-Hyres stability is used to show that the model is UH-stable under the fractal fractional in Atangana-Baleanu sense. The existence theory and Ulam-Hyres stability can be obtained for the other derivatives. The numerical results of the model are obtained via Lagrange piece-wise interpolation. The dynamics of the different compartments of the model are observed via simulations at various values of fractional and fractal orders. Also, the effect of fractal and fractional order is explored by varying fractal and fractional values. Compared with the integer-order or fractional HBV immune delay model, the results of the model under novel operators have more practical significance. Thus, fractal-fractional operators are better tools to explain the dynamics of any physical model.

References

[1] Marion PL , Robinson WS. Hepadna viruses: Hepatitis b and related viruses. *Curr. Top. Microbiol. Immunol.* 105 (1983) 99–121 .
[2] Lavanchy D . Worldwide epidemiology of hbv infection, disease burden, and vaccine prevention. *J. Clin. Virol.* 34 (2005).

[3] Satapathy, P., Gaidhane, S., Bishoyi, A.K., Ganesan, S., Kavita, V., Mishra, S., Kaur, M., Bushi, G., Shabil, M., Syed, R., Puri, S., Kumar, S., Ansar, S., Sah, S., Jena, D., Zahiruddin, Q.S., Goh, K.W. (2025). Burden of acute hepatitis E virus in South Asia: Insights from Global Burden of Disease study 2021. *Diagnostic Microbiology and Infectious Disease*, 112(3).
[4] Dhanasekaran, S., Selvadoss, P.P., Manoharan, S.S., et al. (2024). Regulation of NS5B Polymerase Activity of Hepatitis C Virus by Target Specific Phytotherapeutics: An In-Silico Molecular Dynamics Approach. *Cell Biochemistry and Biophysics*, 82, 2473–2492.
[5] F. Gao, X. Li, W. Li et al., Stability analysis of a fractional-order novel hepatitis B virus model with immune delay based on Caputo-Fabrizio derivative, *Chaos Solitons Fractals* (2020) https://doi.org/10.1016/j.chaos.2020.110436.
[6] J. Zhang, S. Zhang, Application and Optimal Control for an HBV Model with Vaccination and Treatment, *Discrete Dyn. Nat. Soc.* Volume 2018, Article ID 2076983, 13 pages.
[7] Means S, Ali MA, Ho H and Heffernan J, Mathematical Modeling for Hepatitis B Virus: Would Spatial Effects Play a Role and How to Model It? *Front. Physiol.* 11 (2020) 146. doi: 10.3389/fphys.2020.00146.
[8] Zhang S, Zho Y, The analysis and application of an HBV model, *Appl. Math. Model.* 36 (2012) 1302-1312.
[9] de Villiers MJ, Gamkrelidze I, Hallett TB, Nayagam S, Razavi H, Razavi-Shearer D, Modelling hepatitis B virus infection and impact of timely birth dose vaccine: A comparison of two simulation models. *PLoS ONE* 15(8) (2020) https://doi.org/10.1371/journal.pone.0237525.
[10] Khan MA , Farhan M , Islam S , Bonyah E . Modeling the transmission dynamics of avian influenza with saturation and psychological effect. *Discrete Contin Dyn Syst-S* 12(3) (2019) 455–74 .
[11] Ahmad S, Ullah A , Akgül A , Baleanu D. Analysis of the fractional tumour-immune-vitamins model with Mittag–Leffler kernel. *Results Phys.* 19 (2020) 103559.
[12] Ahmad S, Ullah A, Shah K, Akgül A. Computational analysis of the third order dispersive fractional PDE under exponential-decay and Mittag-Leffler type kernels. *Numer Methods Partial Differential Eq* (2020) 1–16. https://doi.org/10.1002/num.22627.
[13] Ahmad S, Ullah A, Arfan M, Shah K. On analysis of the fractional mathematical model of rotavirus epidemic with the effects of breastfeeding and vaccination under Atangana-Baleanu (AB) derivative. *Chaos, Solitons Fractals* 140 (2020) 110233.
[14] Farman M, Akgül A, Ahmad A, Imtiaz S. Analysis and dynamical behavior of fractional-order cancer model with vaccine strategy. *Math. Methods Appl. Sci.* 43(7) (2020) 4871-4882.
[15] Abro KA , Memon AA , Uqaili MA . A comparative mathematical analysis of RL and RC electrical circuits via Atangana-Baleanu and Caputo-Fabrizio fractional derivatives. *Eur Phys J Plus* 133(3) (2018) 113 .
[16] Gómez-Aguilar JF , Torres L , Yépez-Martínez H , Baleanu D , Reyes JM , Sosa IO . Fractional liénard type model of a pipeline within the fractional derivative without singular kernel. *Adv Differ Equ* 2016;2016(1):173 .
[17] K. K. Nisar, S. Ahmad, A. Ullah, K. Shah, H. Alrabaiah, M. Arfan, Mathematical analysis of SIRD model of COVID-19 with Caputo fractional derivative based on real data, *Results Phys.* 21 (2021) 103772.
[18] A.Atangana , D.Baleanu . New fractional derivatives with non-local and non-singular kernel: theory and application to heat transfer model, *Therm Sci* 20(2)(2016) 763–9 .
[19] F. Haq, K. Shah, G. Rahman, M. Shahzad, Numerical analysis of fractional order model of HIV-1 infection of CD4+ T-cells, *Comput. Meth. Differ. Equ.* **5** (1) (2017) 1–11.
[20] Sun HG , Meerschaert MM , Zhang Y , Zhu J , Chen W . A fractal Richards' equation to capture the non-Boltzmann scaling of water transport in unsaturated media. *Adv Water Resour* 52: (2013) 292–5 .
[21] Kanno R . Representation of random walk in fractal space-time. *Physica A* 248 (1998) 165–75 .
[22] Atangana A, Qureshi S. Modelling attractors of chaotic dynamical systems with fractal-fractional operators. *Choas, Solition Fractal* 123(2019):320-337.
[23] Chen W , Sun H , Zhang X , Korosak D . Anomalous diffusion modeling by fractal and fractional derivatives. *Comput Math Appl* 59(5) (2010) 1754–8 .
[24] A. Atangana, Fractal-fractional differentiation and integration: connecting fractal calculus and fractional calculus to predict complex system. *Chaos, Solitons Fractals* 102 (2017) 396–406 .
[25] K. M. Owolabi, A. Atangana, A. Akgulm, Modelling and analysis of fractal-fractional partial differential equations: Application to reaction-diffusion model, *Alex. Eng. J.* 59(2020) 2477–2490.
[26] Z. Ali, F. Rabiei, K. Shah, T. Khodadadi, Fractal-fractional order dynamical behavior of an HIV/AIDS epidemic mathematical model, *Eur. Phys. J. Plus* (2021) 136:36.
[27] B. Ghanbari, On the modeling of the interaction between tumor growth and the immune system using some new fractional and fractional-fractal operators, *Adv. Differ. Equ.* (2020) 2020:585.
[28] Liu, C., Liu, L., Cao, J., Abdel-Aty, M. (2023) Intermittent Event-Triggered Optimal Leader-Following Consensus for Nonlinear Multi-Agent Systems Via Actor-Critic Algorithm, IEEE Transactions on Neural Networks and Learning Systems, 34(8), pp. 3992–4006 http://dx.doi.org/10.1109/TNNLS.2021.3122458
[29] Wang, Z., Cao, J., Lu, G., Abdel-Aty, M. (2020) Fixed-Time Passification Analysis of Interconnected Memristive Reaction-Diffusion Neural Networks, IEEE Transactions on Network Science and Engineering, 7(3), pp. 1814–1824, 8906166 http://dx.doi.org/10.1109/TNSE.2019.2954463
[30] Wang, Z., Cao, J., Cai, Z., Abdel-Aty, M. (2020) A novel Lyapunov theorem on finite/fixed-time stability of discontinuous impulsive systems, Chaos, 2020, 30(1), 013139 http://dx.doi.org/10.1063/1.5121246
[31] Abdel-Aty, M., Moya-Cessa, H. (2007) Sudden death and long-lived entanglement of two trapped ions, Physics Letters A, 369(5-6), pp. 372–376 http://dx.doi.org/10.1016/j.physleta.2007.05.003

[32] Abdalla, M.S., Abdel-Aty, M., Obada, A.-S.F. (2002) Degree of entanglement for anisotropic coupled oscillators interacting with a single atom, Journal of Optics B 4(6), pp. 396–401 http://dx.doi.org/10.1088/1464-4266/4/6/305
[33] Abdel-Aty, M. (2002) General formalism of interaction of a two-level atom with cavity field in arbitrary forms of nonlinearities, Physica A 313(3-4), pp. 471–487 http://dx.doi.org/10.1016/S0378-4371(02)00999-8
[34] Abdalla, M.S., Obada, A.-S.F., Abdel-Aty, M. (2005) Von Neumann entropy and phase distribution of two mode parametric amplifier interacting with a single atom, Annals of Physics, 318(2), pp. 266–285 http://dx.doi.org/10.1016/j.aop.2005.01.002
[35] Abdel-Aty, M., Abdel-Khalek, S., Obada, A.-S.F. (2000) Pancharatnam phase of two-mode optical fields with Kerr nonlinearity, Optical Review, 7(6), pp. 499–504 http://dx.doi.org/10.1007/s10043-000-0499-6
[36] Obada, A.-S.F., Abdel-Hafez, A.M., Abdelaty, M. (1998) Phase properties of a Jaynes-Cummings model with Stark shift and Kerr medium, European Physical Journal D, 3(3), pp. 289–294 http://dx.doi.org/10.1007/s100530050176